

**Group II truncated haemoglobin Yjbl prevents reactive oxygen species-induced protein aggregation in *Bacillus subtilis***

Takeshi Imai<sup>1\*</sup>, Ryuta Tobe<sup>2</sup>, Koji Honda<sup>1</sup>, Mai Tanaka<sup>2</sup>, Jun Kawamoto<sup>3</sup>, and Hisaaki Mihara<sup>2\*</sup>

<sup>1</sup>Hyogo Prefectural Institute of Technology, Kobe 654-0037, Hyogo, Japan

<sup>2</sup>Department of Biotechnology, Ritsumeikan University, Kusatsu 525-8577, Shiga, Japan

<sup>3</sup>Institute for Chemical Research, Kyoto University, Uji 611-0011, Kyoto, Japan

**\*Corresponding authors:** imai@hyogo-kgt.ac.jp and mihara@fc.ritsumei.ac.jp

**Abbreviations:** ROS, reactive oxygen species; trHb, truncated haemoglobin; BSA, bovine serum albumin; BSA-OOH, hydroperoxidised BSA; AAPH, 2,2'-azobis(2-amidinopropane) dihydrochloride;

**Abstract**

Oxidative stress-mediated formation of protein hydroperoxides can induce irreversible fragmentation of the peptide backbone and accumulation of cross-linked protein aggregates, leading to cellular toxicity, dysfunction, and death. However, how bacteria protect themselves from damages caused by protein hydroperoxidation is unknown. Here we show that Yjbl, a group II truncated haemoglobin from *Bacillus subtilis*, prevents oxidative aggregation of cell-surface proteins by its protein hydroperoxide peroxidase-like activity, which removes hydroperoxide groups from oxidised proteins. Disruption of the *yjbl* gene in *B. subtilis* lowered biofilm water repellence, which associated with the cross-linked aggregation of the biofilm matrix protein TasA. Yjbl was localised to the cell surface or the

26 biofilm matrix, and the sensitivity of planktonically grown cells to generators of reactive  
27 oxygen species was significantly increased upon *yjbI* disruption, suggesting that YjbI  
28 pleiotropically protects labile cell-surface proteins from oxidative damage. YjbI removed  
29 hydroperoxide residues from the model oxidized protein substrate bovine serum albumin and  
30 biofilm component TasA, preventing oxidative aggregation *in vitro*. Furthermore, the  
31 replacement of Tyr<sup>63</sup> near the haem of YjbI with phenylalanine resulted in the loss of its  
32 protein peroxidase-like activity, and the mutant gene failed to rescue biofilm water repellency  
33 and resistance to oxidative stress induced by hypochlorous acid in the *yjbI*-deficient strain.  
34 These findings provide new insights into the role of truncated haemoglobin and the  
35 importance of hydroperoxide removal from proteins in the survival of aerobic bacteria.

36

## 37 **Introduction**

38 Truncated haemoglobins (trHbs) are small haem proteins found in microbes and plants  
39 (Wittenberg et al., 2002, Boechi et al., 2010). They belong to the globin superfamily and  
40 form a distinct family separated from bacterial flavohemoglobins, *Vitreoscilla* haemoglobin,  
41 plant symbiotic and non-symbiotic haemoglobins, and animal haemoglobins (Vuletich and  
42 Lecomte, 2006, Boechi et al., 2010). The haem group enables trHbs to bind to small  
43 biomolecules, such as oxygen (O<sub>2</sub>), carbon monoxide (CO), and nitric oxide (NO)  
44 (Wittenberg et al., 2002). Additionally, haem-pocket residues are highly structurally variable,  
45 conferring trHbs with diverse roles, such as scavengers (Ouellet et al., 2002) or transport  
46 carriers (Liu et al., 2004, Wittenberg et al., 2002) of the corresponding small ligands. Such  
47 versatility is possibly related to defence mechanisms against the harmful effects of reactive  
48 oxygen species (ROS). trHbs are also implicated in the pathogenicity of some bacteria  
49 (Pawaria et al., 2007, Ascenzi et al., 2008, Wittenberg et al., 2002), but the molecular  
50 functions of these proteins are unclear.

51 The trHb family proteins are further divided into three subfamilies, Groups I (trHbN),  
52 II (trHbO), and III (trHbP), with each subfamily having different structural characteristics  
53 (Bustamante et al., 2016, Wittenberg et al., 2002). Among these subfamilies, trHbO proteins  
54 evolutionarily originated before trHbN and trHbP proteins and are distributed into  
55 Actinobacteria, Proteobacteria, Firmicutes, and plants (Vuletich and Lecomte, 2006, Boechi  
56 et al., 2010). A trHbO from *Mycobacterium tuberculosis* exhibits inefficient gas-exchange  
57 capacity with a very slow release of O<sub>2</sub> (Ouellet et al., 2003) and a slower reaction rate with  
58 NO than other trHb subfamilies (Ouellet et al., 2003), suggesting that trHbOs play additional  
59 roles other than transporting these molecules (Giangiacomo et al., 2005). In accordance,  
60 trHbOs from *M. tuberculosis* (Ouellet et al., 2007), *Thermobifida fusca* (Torge et al., 2009),  
61 and *Roseobacter denitrificans* (Wang et al., 2015) can exhibit peroxidase activity on

62 hydrogen peroxide *in vitro*. However, because these bacteria express catalases that scavenge  
63 hydrogen peroxide (Manca et al., 1999), the physiological relevance of the peroxidase  
64 activity of trHbOs remains unknown.

65         The Gram-positive bacterium *Bacillus subtilis* possesses a trHbO, termed YjbI. YjbI  
66 has been heterologously expressed as a recombinant protein in *Escherichia coli*, and the  
67 purified protein has been characterised (Choudhary et al., 2005). It exists as a monomer with  
68 a molecular mass of 15.1 kDa and comprises 132 amino acid residues (Choudhary et al.,  
69 2005). The three-dimensional crystal structure of YjbI in the form of the cyano-Met  
70 derivative was determined at 2.15-Å resolution (Giangiacomo et al., 2005), revealing  
71 intriguing structural features, including a shallow depression on the proximal side of the  
72 haem. The binding properties of YjbI to O<sub>2</sub> (Boechi et al., 2010, Ouellet et al., 2002), CO  
73 (Boechi et al., 2010, Ouellet et al., 2002, Choudhary et al., 2005, Feis et al., 2008, Lapini et  
74 al., 2012), and hydrogen sulphide (Nicoletti et al., 2010) have been extensively studied *in*  
75 *vitro*. Some have observed that YjbI has a high affinity for O<sub>2</sub> and hydrogen sulphide, and the  
76 oxygenated derivative is significantly stable, which may rule out a role of YjbI in O<sub>2</sub>  
77 transport/storage. As is common for many haem proteins, an inherent low peroxidase activity  
78 of YjbI on hydrogen peroxide has been reported (Choudhary et al., 2005), but this  
79 observation remains controversial. The *yjbI* gene is part of the *yjbIH* operon. YjbH is a  
80 bacterial adaptor protein required for efficient degradation of the disulphide-stress-activated  
81 transcription regulator Spx by the protease ClpXP (Larsson et al., 2007, Awad et al., 2019).  
82 Although these previous studies have implied a possible link between YjbI and response to  
83 oxidative stress, the exact function of YjbI remains unclear.

84         In this study, we present *in vivo* and *in vitro* analyses of the physiological function of  
85 *B. subtilis* YjbI. We show *yjbI* is required for the formation of biofilms with water repellence.  
86 YjbI was found to suppress the ROS-mediated aggregation of the major biofilm matrix



87 protein TasA and localise to the bacterial cell surface or the biofilm matrix. We show that,  
88 besides a role in biofilm maintenance, YjbI functions as an antioxidant protein. Moreover, we  
89 observed YjbI exerted a peroxidase-like activity on a protein hydroperoxide substrate. YjbI is  
90 proposed to function as an antioxidant protein in protecting cell-surface proteins from ROS-  
91 induced aggregation via its protein hydroperoxide peroxidase-like activity.

92

## 93 **Results**

### 94 ***yjbI* is required for normal formation of the *B. subtilis* biofilm**

95 We observed unusual biofilm formation by the *yjbI*-deficient mutant on a solid medium.  
96 Specifically, the *B. subtilis* 168 WT strain formed architecturally complex colonies with  
97 characteristic wrinkles on the MSgg solid medium, whereas the *yjbI*-deficient mutant failed  
98 to establish such biofilms; instead, it formed flat and glossy colonies (Fig. 1a). Because of the  
99 water-repellent properties of the mature biofilm surfaces, the functional integrity of a biofilm  
100 can be inferred from the contact angle of a water droplet placed on top of the biofilm  
101 (Arnaouteli et al., 2017, Arnaouteli et al., 2016, Kobayashi and Iwano, 2012). Through this  
102 method, we examined the integrity of the biofilms of the *yjbI*-deficient mutant. Water  
103 droplets placed on the surfaces of the WT biofilms assumed nearly spherical shapes with a  
104 contact angle of  $116 \pm 4.12^\circ$ , indicating the remarkable surface repellence of the WT biofilms  
105 (Fig. 1a). In contrast to the WT strain, the water droplets on the surfaces of *yjbI*-deficient  
106 mutant biofilms had a contact angle of  $30 \pm 1.55^\circ$ , indicating a significant loss of surface  
107 repellence in the deficient mutant biofilms. Similarly, the *tasA*-deficient mutant (COTNd,  
108 Supplementary File 1), which was a negative control lacking TasA, the main fibrous protein  
109 in *B. subtilis* biofilms (Diehl et al., 2018, Hobley et al., 2015, Romero et al., 2010), failed to  
110 form biofilms with normal wrinkles and water repellence (Fig. 1a). When *yjbI* was  
111 reintroduced into the *yjbI*-deficient mutant, the ability of the strain to form biofilms with

wrinkles and surface repellence was markedly recovered (Fig. 1a). These results indicated that Yjbl is required for normal biofilm formation.

### **Yjbl suppresses ROS-mediated TasA aggregation**

Since the *yjbl*-deficient mutant lost the biofilm surface repellence in a manner like that of the *tasA*-deficient mutant, we examined the effect of *yjbl* deficiency on TasA. His-tagged TasA (TasA-His) was expressed in the WT and *yjbl*-deficient strains carrying pHtasA1 by cultivating in the biofilm-promoting liquid MSgg medium, and the soluble and insoluble protein fractions from the lysate of the pellicles of each strain were analysed by SDS-PAGE followed by western blotting using an anti-His-tag antibody. A band with the expected molecular mass of 31 kDa for TasA-His was detected in the soluble fractions from both the WT and *yjbl*-deficient strains (Fig. 2a). The 31-kDa TasA-His band was also detected in the insoluble fraction from the WT strain (Fig. 2a). In contrast, we observed smeared bands with markedly high molecular masses (> 225 kDa) in the insoluble fraction from the *yjbl*-deficient mutant (Fig. 2a), suggesting that Yjbl prevents TasA from forming high-molecular-mass aggregates. No monomeric TasA was detected in the insoluble fraction of the *yjbl*-deficient mutant strain. An aggregate of TasA was observed under strong reducing and heat-denaturing conditions in SDS sample buffer, suggesting that covalent bonds may be involved in aggregate formation.

Covalent cross-linking of proteins is generally known to be caused by ROS-mediated protein oxidation (Davies, 2016, Gebicki, 1997, Dean et al., 1997). We could partly reproduce the TasA aggregation *in vitro* by oxidising purified TasA<sub>28-261</sub>-His (a mature form of TasA with a C-terminal His-tag) at neutral pH in the presence of hydrogen peroxide and Fe<sup>2+</sup>, which undergo the Fenton reaction (Gebicki, 1997, Welch et al., 2002). The Fenton reaction produces hydroxyl radicals according to the following equation:  $\text{Fe}^{2+} + \text{H}_2\text{O}_2 \rightarrow \text{Fe}^{3+}$

+ OH<sup>-</sup> + ·OH, and was used to induce ROS-mediated protein oxidation. We investigated whether YjbI could prevent this oxidation-induced aggregation and found that adding purified YjbI (Figure 2-figure supplement 1) to the mixture significantly suppressed the formation of TasA<sub>28-261</sub>-His aggregates (Fig. 2b), consistent with the results of the *in vivo* experiment shown in Figure 2a. These findings suggest YjbI suppresses ROS-mediated TasA aggregation.

#### **YjbI localises to the cell surface or the biofilm matrix of *B. subtilis***

TasA localises to the cell surface by the Sec pathway (Romero et al., 2010, Romero et al., 2011). Because YjbI suppressed TasA aggregation *in vivo* (Fig. 2a), it is reasonable to expect that YjbI also localises to the cell surface. To address this hypothesis, the soluble and insoluble fractions of cell lysates from WT and *yjbI*-deficient *B. subtilis* pellicles and the planktonically grown culture supernatants were analysed by western blotting using an anti-YjbI antiserum. YjbI was detected only in the insoluble fraction from the WT pellicles (Fig. 2c). We then examined whether YjbI is exposed on the cell surface. Toward this end, we treated intact *B. subtilis* WT pellicles with a protease cocktail before western blot analysis of the whole cells. The protease treatment almost eliminated the immunoreactive YjbI from the intact *B. subtilis* WT pellicles, suggesting that YjbI is localised to the extracellular surface (Fig. 2d). Furthermore, we examined whether YjbI could be recognised by anti-YjbI antibodies, which must be cell impermeable. Treatment of the intact WT cells with the anti-YjbI antiserum before cultivation on MSgg medium impaired colony biofilm formation, with a significant loss of surface repellence (Fig. 2e), as observed for the *yjbI*-deficient mutant. In contrast, treatment with the control pre-immune serum showed almost no effect. These observations suggest that anti-YjbI antibodies can interact with YjbI to impair its function on

the biofilm surface. Taken together, these results suggest that YjbI localises to the cell surface or the biofilm matrix of *B. subtilis*.

### **YjbI functions as an antioxidant protein in *B. subtilis***

To address whether YjbI functions exclusively in biofilm maintenance or in a general cellular protection against oxidative stress, we analysed the effect of 2,2'-azobis(2-amidinopropane) dihydrochloride (AAPH)-induced oxidative stress on the planktonic growth of *B. subtilis* strains in lysogeny broth (LB) liquid medium under shaking conditions. AAPH was chosen as the radical initiator because it gently generates free radicals under neutral pH (Gebicki and Gebicki, 1993) and is suitable for a long-term cultivation experiment. We observed no significant difference between the WT strain and *tasA*-deficient mutant in the sensitivity to AAPH, indicating that TasA plays no apparent role in the protection of the planktonically grown cells from oxidative stress (Fig. 2f). In contrast, the *yjbI*-deficient mutant showed hypersensitivity to AAPH compared with the WT and *tasA*-deficient mutant (Fig. 2f). This result shows that the hypersensitivity of the *yjbI*-deficient mutant to AAPH is not because of TasA impairment in this mutant but presumably because YjbI is involved in a general cellular protection against AAPH-induced oxidative stress, at least during the planktonic growth. Interestingly, disruption of *yjbH* (BKE11550, Supplementary File 1), which is co-transcribed with *yjbI* (Rogstam et al., 2007), did not alter the sensitivity to AAPH-induced oxidative stress (Fig. 2f), suggesting that YjbI functions independently of YjbH under oxidative stress.

The effect of the oxidative stress induced by hypochlorous acid (HClO) on the *yjbI*-deficient mutant was also examined. HClO is a strong bactericidal agent that can cause severe protein hydroperoxidation via the generation of radicals on amino acid residues (Hawkins and Davies, 1998, Stadtman and Levine, 2003). A minimum bactericidal concentration assay revealed that the sensitivity of the *yjbI*-deficient mutant to hypochlorous acid was

approximately 100 times higher than the WT strain (Table 1). These data demonstrate that the loss of *yjbI* increases the sensitivity of the cells to oxidative stress, suggesting that YjbI functions as a powerful antioxidant protein in *B. subtilis*. Taken together, these results suggest that the antioxidant role of YjbI is not limited to maintaining the function of TasA in biofilm formation; most likely, YjbI functions to protect any labile cell-surface protein from oxidative damage.

### **YjbI exhibits protein hydroperoxide peroxidase-like activity**

The observed ROS-mediated TasA aggregation likely involves intermolecular covalent cross-linking among individual TasA proteins (Fig. 2a and 2b). Protein cross-links are formed via radical reactions and the Michael additions after the generation of protein hydroperoxides (half-life: ~4 h at 37 °C) (Davies, 2016), (Gieseg et al., 2000) (Fig. 3a). Therefore, we examined *in vitro* whether YjbI could prevent the ROS-mediated aggregation of bovine serum albumin (BSA), which has been a model protein in studies of protein hydroperoxides (Gebicki and Gebicki, 1993). A hydroperoxidised BSA (BSA-OOH) was prepared using the Fenton reaction followed by removal of excess hydrogen peroxide and unstable radicals via cold acetone precipitation (Gieseg et al., 2000). Subsequent incubation of BSA-OOH in the absence of YjbI promoted the spontaneous self-crosslinking of BSA to yield BSA aggregates and a concomitant fragmentation via nonspecific free radical chain reactions (Fig. 3a) (Fig. 3b). In contrast, the addition of YjbI to the subsequent incubation of BSA-OOH markedly suppressed the BSA-OOH aggregation (Fig. 3b). An identical result was obtained for BSA-OOH prepared using AAPH (Fig. 3c). The protective function against oxidative BSA aggregation/fragmentation was specific to YjbI, because two typical haem proteins, haemoglobin, and myoglobin, showed no protective effects, but promoted the oxidative BSA aggregation/fragmentation (Fig. 3d). The effects of haemoglobin and myoglobin are

consistent with a previous observation that coexistence of a haem group and an oxidant generally accelerates radical reactions (Svistunenko, 2005). Time course analysis further demonstrated the rapid and significant elimination of the hydroperoxide groups from BSA-OOH by YjbI (Fig. 3e). To provide direct experimental evidence of the proposed link between TasA and YjbI, we purified mature TasA (Figure 3-figure supplement 1) and prepared TasA-OOH using the same procedure as for BSA-OOH. The addition of YjbI to TasA-OOH significantly decreased its hydroperoxide groups (Fig. 3f), as observed in BSA-OOH. Taken together, these results suggest that YjbI prevents protein aggregation/fragmentation, most likely through its haem-mediated protein hydroperoxide peroxidase-like activity (Fig. 3a).

### **Effect of amino acid substitution in YjbI on its *in vivo* and *in vitro* functions**

We investigated whether phenotypic abnormalities in biofilms were related to the structure near the possible active center of YjbI. Point mutations were introduced into electron-rich residues near the haem of YjbI to produce its derivatives, Y25F, Y63F, and W89F. Each plasmid expressing one of these derivatives was introduced into a *yjbI*-deficient strain and examined for biofilm integrity. The results showed that water repellence in the *yjbI*-deficient strain was not rescued by the introduction of Y63F, while Y25F and W89F complemented the *yjbI*-deficient phenotype (Fig. 4a). This result indicates that Tyr<sup>63</sup> is important for YjbI function. Furthermore, HClO resistance was partially restored by the introduction of a plasmid-encoded wild-type *yjbI* gene (*yjbI*<sup>WT</sup>) into the *yjbI*-deficient strain (Table 2). Among the mutant strains complemented with the *yjbI* derivatives, *yjbI*/*yjbI*<sup>W89F</sup> strain recovered its HClO resistance to the same extent as the *yjbI*/*yjbI*<sup>WT</sup>, whereas both *yjbI*/*yjbI*<sup>Y25F</sup> and *yjbI*/*yjbI*<sup>Y63F</sup> mutants showed high sensitivity to HClO, similar to the *yjbI*-deficient mutant. The apparent discrepancy between the biofilm water repellence and the HClO sensitivity of *yjbI*

/yjbI<sup>Y25F</sup> may be due to differences in experimental conditions, such as the levels of oxidative stress and the type of growth (biofilms or planktonic). To determine whether the significant phenotypic changes observed for yjbI/yjbI<sup>Y63F</sup> relate to the protein hydroperoxide peroxidase-like activity of YjbI, we purified the Y63F derivative (Figure 4-figure supplement 1) and evaluated its ability to remove the hydroperoxide groups in BSA-OOH. We found that Y63F lost its hydroperoxide peroxidase-like activity (Fig. 4b). Tyr<sup>63</sup> was also conserved in *M. tuberculosis* trHbO, and this residue has been predicted to interact with haem most significantly (Ouellet et al., 2007). Our results clearly indicate that Tyr<sup>63</sup> is important for both the *in vivo* and *in vitro* functions of YjbI, suggesting that its protein hydroperoxide peroxidase-like activity is linked to the maintenance of biofilm integrity.

#### **YjbI does not affect lipid peroxidation**

Lipids, one of the cell-surface components, are also hydroperoxidised by ROS (Cabiscol et al., 2000). We examined whether yjbI disruption also affects the amount of lipid hydroperoxides in biofilms. The colony biofilms of the WT and yjbI-deficient strains were prepared on solid MSgg medium, and the amounts of lipid hydroperoxide in the collected biofilms were determined. Therefore, the level of lipid hydroperoxide was not significantly increased in the yjbI-deficient mutant relative to the level in the WT, implying that YjbI does not function in eliminating lipid hydroperoxides (Figure 3-figure supplement 2).

#### **Discussion**

In this study, we revealed a physiological and biochemical function of YjbI. Our results suggest YjbI prevents the ROS-induced aggregation of proteins, such as TasA, localised on the cell surface of *B. subtilis*. We also showed that YjbI may possess a unique protein hydroperoxide peroxidase-like activity, absent from other haem proteins, such as

haemoglobin and myoglobin. Oxidative protein aggregation and protein carbonyls derived from protein radicals and hydroperoxides (Davies, 2016) have emerged as important biomarkers of various cellular defects caused by oxidative stress not only in mammals (Korovila et al., 2017, Heinecke et al., 1993) but also in bacteria (Ling et al., 2012). Peroxiredoxins have been reported to repair intracellular protein peroxidation in mammals (Peskin et al., 2010). However, Yjbl is distinct from peroxiredoxins in that it is a haem protein with no significant sequence homology (<15%). The second-order rate constants ( $M^{-1} \cdot s^{-1}$ ) for the reactions of mammalian peroxiredoxins 2 and 3 with BSA-OOH are 160 and 360, respectively, and have been shown to reduce protein hydroperoxides more efficiently than GSH under physiological conditions (Peskin et al., 2010). Although direct comparison is difficult due to different experimental conditions, Yjbl and peroxiredoxins are likely to have a similar catalytic rate, as both proteins can reduce BSA-OOH in the order of several  $\mu M$  in roughly 5 min at similar protein concentrations (Fig. 3e) (Peskin et al., 2010). Interestingly, selenomethionine can catalyze the removal of hydroperoxides from proteins in the presence of GSH or a thioredoxin system (Rahmanto & Davies, 2011). However, this system, as well as peroxiredoxins, localises in the cytoplasm of cells, which is a significant difference between Yjbl and these proteins. Moreover, whether bacteria utilize peroxiredoxins and the selenomethionine system to remove hydroperoxides from proteins remains unclear.

Most studies on biofilm formation in *B. subtilis* use the *B. subtilis* NCBI3610 strain as a model bacterium because of its ability to form well-structured three-dimensional biofilms (Arnaouteli et al., 2021, Mielich-Süss et al., 2014). The biofilms of the wild-type and *tasA* mutant strains of the *B. subtilis* 168 strain are known to be morphologically different from those of the *B. subtilis* NCBI3610 strain (Romero et al., 2010, Vlamakis et al., 2008, Erskine et al., 2018). In this study, the *B. subtilis* 168 strain was used because it is the most representative of *B. subtilis* and serves as a model organism for a wider range of research



aspects (Zeigler et al., 2008) as we were not only interested in evaluating biofilm formation but also in more general aspects of oxidative damage responses in bacteria.

In *B. subtilis*, several cytosolic factors have been known to protect the cells from oxidative damages. The catalase KatA (Chen et al., 1995) and hydrogen peroxide peroxidase AhpC (Broden et al., 2016) protect the cells from hydrogen-peroxide-induced oxidative damages. OhrA and OhrB contribute to the cellular protection from organic hydroperoxides (Fuangthong et al., 2001). In addition, bacillithiol has been proposed to be involved in superoxide stress and metal homeostasis, but not in hydrogen-peroxide-induced oxidative stress (Fang and Dos Santos, 2015, Gaballa et al., 2010). However, much less is known about the mechanism protecting cell-surface proteins from oxidative damages in Gram-positive bacteria. In the Gram-positive *Streptococcus pneumoniae*, surface-exposed proteins with methionine sulfoxide residues are reduced by the membrane-bound methionine sulfoxide reductase MsrAB2 (Saleh et al., 2013), but the gene of an equivalent membrane-anchored enzyme is absent from the *B. subtilis* genome. To our best knowledge, YjbI is the first example of an antioxidant protein involved in protecting cell-surface proteins against oxidative aggregation. Antioxidation of cell-surface proteins is important, especially for proteins located and exposed at the air-liquid interface, such as the biofilm surface (Beloin et al., 2004, Ezraty et al., 2017). Disrupting *yjbI* had a crucial effect on the integrity of the biofilm cell surface, presumably because of this reason (Fig. 1).

*M. tuberculosis* trHbO has an autokinase activity and plays a role in the survival and adaptation of the bacterium under hypoxia (Hade et al., 2020). However, *M. tuberculosis* trHbO shares a moderate (31%) amino acid sequence identity with *B. subtilis* YjbI, and *M. tuberculosis* carries another truncated haemoglobin, trHbN (Couture et al., 1999), which is missing in *B. subtilis*. Moreover, because *M. tuberculosis* is an obligate aerobic bacterium, its responses under oxygen stress may be largely different from those of the member of the

311 facultative anaerobes *B. subtilis*. Whether the YjbI orthologues found in other bacteria,  
312 including other *B. subtilis* strains, function in the suppression of oxidative protein  
313 aggregation, biofilm formation, or oxidant resistance remains an open question for future  
314 research.

315 In this study, we demonstrated YjbI reduces hydroperoxide groups in BSA-OOH via  
316 its peroxidase-like activity and suppressed the spontaneous aggregation of BSA-OOH.  
317 Typical haem peroxidases, such as horseradish peroxidase and lactoperoxidase, exhibit  
318 negligible activity on protein hydroperoxides (Davies, 2016, Morgan et al., 2004, Gebicki et  
319 al., 2002). Haemoglobin and myoglobin can react with small peptide-sized hydroperoxides  
320 but not with large protein hydroperoxides, such as BSA-OOH (Morgan et al., 2004). The X-  
321 ray crystal structure of *B. subtilis* YjbI (PDB ID: 1UX8) (Giangiacomo et al., 2005) shows  
322 this protein has a 55-Å<sup>2</sup> surface opening (Figure 3-figure supplement 3), which may allow  
323 direct access of bulk solvent and large molecules to the haem active-site. Therefore, the  
324 structural feature probably confers the potential to react with a protein hydroperoxide on YjbI.

325 An electron donor is required for the proposed protein hydroperoxide peroxidase-like  
326 reaction by YjbI. We showed that the *in vitro* reduction of BSA-OOH and TasA-OOH by  
327 YjbI proceeded without addition of any external electron donors (Fig. 3). This observation  
328 implies that electrons needed for the *in vitro* protein hydroperoxide peroxidase-like reaction  
329 may be provided from the amino acid residues of YjbI itself. Interestingly, in the hydrogen  
330 peroxide peroxidase reaction catalysed by *M. tuberculosis* trHbO, the tyrosine residues near  
331 the haem of trHbO have been suggested to serve as electron donors (Ouellet et al., 2007). At  
332 least two of these tyrosine residues are conserved in trHbO orthologues (Tyr<sup>25</sup> and Tyr<sup>63</sup> in  
333 YjbI), which are located close to the haem according to the results of the crystal structure  
334 analysis (Giangiacomo et al., 2005). In addition, tryptophan, another electron-rich amino acid  
335 residue, is thought to contribute to electron transfer in the *M. tuberculosis* trHbO ortholog

(Trp<sup>89</sup> in YjbI) (Ouellet et al., 2007). In particular, tyrosine can be stabilised by providing electrons to yield either dityrosine or a series of oxidised derivatives of dityrosine, 3,4-dihydroxyphenylalanine (DOPA), DOPA semiquinone, and DOPA quinone (Maskos et al., 1992, Giulivi and Davies, 2001). In fact, as shown in this study, the mutation in Tyr<sup>63</sup> affected the phenotype of *B. subtilis* (Fig. 4a, Table 2) and the activity of YjbI (Fig. 4b). Taken together, we propose that the tyrosine residues in YjbI are the most promising candidates for donating electrons for the *in vitro* YjbI-catalysed protein hydroperoxide peroxidase-like reaction. Nevertheless, it remains unclear whether YjbI utilises an endogenous or exogenous electron donor other than the amino acid residues of YjbI itself *in vivo*. Previous reports have shown that *M. tuberculosis* trHbO can receive electrons from ferrocycytochrome *c* (Ouellet et al., 2007). Alternatively, YjbH, a DsbA-like protein (Guddat et al., 1998) with two active-site cysteine residues, may have a potential to donate electrons for the YjbI-catalysed reduction of protein hydroperoxides (Fabianek et al., 2000). However, the role of YjbH as an electron donor to YjbI is inconclusive because disrupting *yjbH* did not affect the sensitivity to AAPH (Fig. 2f), and YjbH localises to the cytosol, unlike YjbI, to function as an effector of Spx, a central regulator of stress response (Larsson et al., 2007). It is also possible that physiological electron donation is operated by more than one molecule, as typical haem proteins can utilise a variety of electron-rich small or large molecules as electron donors because of their wide substrate specificity (Galaris et al., 1989) (Hayashi et al., 1999) (Ouellet et al., 2007).

The localisation of YjbI to the cell surface or the biofilm matrix is consistent with its role in protecting TasA and other cell-surface proteins from ROS-induced aggregation (Fig. 5a and 5b). However, there is no apparent targeting signal sequence in the amino acid sequence of YjbI, and bioinformatic analysis using SignalP (<http://www.cbs.dtu.dk/services/SignalP/abstract.php>) or PSORT (<https://www.psорт.org>)

361 predicted that YjbI is a cytoplasmic protein (Figure 5-figure supplement 1). Purified  
362 recombinant YjbI, which was produced in *E. coli*, was obtained in a soluble form (Figure 2-  
363 figure supplement 1), in contrast to the insoluble feature of the native YjbI in *B. subtilis*.  
364 Analogously, *M. tuberculosis* trHbN belonging to another group of trHb family, is also  
365 devoid of a targeting signal sequence, is localised to the cell surface following glycosylation,  
366 whereas the corresponding recombinant protein expressed in *E. coli* is detected in a soluble  
367 form (Arya et al., 2013). Nevertheless, no glycosylation site is found on YjbI. Therefore, the  
368 mechanism for the translocation of YjbI to the extracellular surface or the biofilm matrix  
369 should be investigated in future studies.

370         Although protein hydroperoxides are one of the major products formed because of  
371 ROS-mediated protein oxidation (Davies et al., 1995, Gebicki, 1997), (Gebicki and Gebicki,  
372 1999), little is known about the effects of their generation on bacterial physiology. Biofilm  
373 matrix proteins are expected to be exposed to an air-liquid interface, which is a region with a  
374 relatively high risk of protein oxidation. Therefore, repairing the oxidatively damaged  
375 proteins on the cell surface may be important for bacterial adaptation in oxidative  
376 environments. The loss of biofilm integrity associated with the irreversible aggregation of the  
377 biofilm matrix protein TasA in the *yjbI*-deficient strain may provide an important clue to  
378 further understand the significance of protein hydroperoxide generation on the cell surface.

379         The findings of this study may lead to future applications. An increasing number of  
380 studies have suggested that biofilms are associated with bacterial infections in humans and  
381 with natural resistance of pathogenic bacteria to antibiotics (Hall and Mah, 2017). We found  
382 that *B. subtilis* biofilm formation can be suppressed by an antiserum against YjbI (Fig. 2e)  
383 and that YjbI deficiency severely impairs the bacterial tolerance to the oxidative stress  
384 induced by AAPH (Fig. 2d) or HClO (Table 1). HClO oxidises various amino acid residues  
385 such as methionine and lysine. In addition, the reaction of HClO with O<sub>2</sub> helps to form

hydroxy radicals (Candeias et al., 1993, Candeias et al., 1994), which initiates protein peroxidation (Stadtman and Levine, 2003). Intriguingly, leukocytes employ ROS, including peroxides and HClO, in the respiratory burst during the innate immune response to bacterial infection (Babior, 1984). Therefore, the YjbI orthologues in pathogenic bacteria would be potential novel drug targets to inhibit pathogenic bacterial growth and biofilm formation. In fact, trHbO is implicated in *Mycobacterium* pathogenicity (Wittenberg et al., 2002). Future studies on the structure-function relationship of YjbI may contribute to developing a specific inhibitor that suppresses infections by the wide variety of trHbO-harboursing pathogenic bacteria (e.g., *Bacillus*, *Mycobacterium*, and *Staphylococcus*).

## **Methods**

### **Bacterial strains, plasmids, and culture conditions**

The bacterial strains and plasmids used in this study are listed in Supplementary File 1. *B. subtilis* 168 and *E. coli* derivatives were obtained by transformation of competent cells with plasmids according to standard protocols (Harwood and Cutting, 1990, Studier and Moffatt, 1986). For pre-cultivation, *B. subtilis* strains were grown in LB medium at 37 °C for 8 h. Recombinant *E. coli* strains were cultivated in LB medium at 37 °C. When appropriate, 30 µg/mL tetracycline and 100 µg/mL kanamycin were added to the cultures of *B. subtilis* and *E. coli*, respectively.

### **Pellicles and colony biofilm formation**

Pellicles in liquid media were prepared by inoculating 1/20 volume of the *B. subtilis* pre-culture in the biofilm-promoting MSgg medium (Bucher et al., 2016) (5 mM potassium phosphate in 100 mM MOPS buffer at pH 7.0 supplemented with 2 mM MgCl<sub>2</sub>, 700 µM CaCl<sub>2</sub>, 50 µM MnCl<sub>2</sub>, 50 µM FeCl<sub>3</sub>, 1 µM ZnCl<sub>2</sub>, 2 µM thiamine, 0.5% (w/w) glycerol, 0.5%

(w/w) glutamate, 0.005% (w/w) phenylalanine, 0.005% (w/w) tryptophan, and 0.005% (w/w) threonine), followed by cultivation at 37 °C for 48 h without shaking. Bacterial colony biofilms on a solid medium were obtained by inoculating a 3-μL aliquot of the *B. subtilis* pre-culture on solid MSgg medium containing 1.5% (w/w) agar, followed by cultivation at 37 °C for 48 h.

#### **Biofilm surface repellence analysis**

Biofilm surface repellence was evaluated according to a described method (Arnaouteli et al., 2017) by measuring the contact angle of a 2-μL water droplet placed on the centre of a bacterial colony biofilm formed on solid MSgg medium, using a DSA100 drop shape analyser (KRÜSS). The water droplet was equilibrated at 28 °C for 5 min before imaging and measurement. The contact angle is presented as the mean ± SEM of at least three independent experiments.

#### **Fractionation of soluble and insoluble *B. subtilis* biofilm proteins**

*B. subtilis* pellicle (0.1 g) was harvested using a spatula and lysed by incubation with 0.5 mL of B-PER (Thermo Fisher Scientific) saturated with phenylmethylsulfonyl fluoride (PMSF, Sigma-Aldrich), supplemented with 5 mg/mL lysozyme at 28 °C for 2 h, and centrifuged. Both the soluble proteins in the supernatant and the precipitated insoluble proteins were recovered and used for further studies.

#### **Purification of YjbI and TasA produced in *E. coli***

To purify recombinant YjbI, *E. coli* BL21(DE3)/pEyjbI2 cells (Supplementary File 1) were grown in LB medium at 37 °C for 6 h, followed by induction of gene expression with 25 μM isopropyl β-D-1-thiogalactopyranoside and further cultivation for 10 h. After centrifugation,

436 harvested cells were lysed in B-PER (Thermo Fisher Scientific) supplemented with  
437 approximately 1 mM PMSF according to the manufacturer's instructions. After  
438 centrifugation, the crude extract was fractionated with ammonium sulphate (30–60%  
439 saturation) for 16 h at 4 °C. After centrifugation, the protein precipitate was resuspended in  
440 50 mM MOPS buffer (pH 7.0) and then applied to a Sephacryl S-100 column (GE  
441 Healthcare) equilibrated with the same buffer. Red haemoprotein fractions from the column  
442 were collected and passed through an Amicon Ultra 100 kDa device (Millipore). The filtrate  
443 containing YjbI was applied to a Toyopearl DEAE-650M column (Tosoh) equilibrated with  
444 50 mM Tris-acetate buffer (pH 7.4). YjbI was eluted at a flow rate of 0.25 mL/min with a  
445 linear NaCl gradient (0–0.5 M) prepared in the same buffer. The fractions containing YjbI  
446 were desalted and concentrated using an Amicon Ultra 10 kDa device in 50 mM Tris-acetate  
447 buffer (pH 7.4) to yield the purified YjbI preparation.

448 His-SUMO-YjbI(Y63F) and His-SUMO-TasA<sub>28-261</sub> were produced in *E. coli*  
449 BL21(DE3)/pEyjbI3 and *E. coli* BL21(DE3)/pEtasA3, respectively (Supplementary File 1)  
450 and cultured in LB medium at 37°C for 6 h, followed by induction with 25 µM isopropyl β-  
451 D-1-thiogalactopyranoside and further cultivation for 10 h. Cells were harvested by  
452 centrifugation and lysed with B-PER (Thermo Fisher Scientific) supplemented with  
453 approximately 1 mM PMSF. The crude extract was applied to an immobilized metal affinity  
454 chromatography (IMAC) resin charged with cobalt (HisTALON Gravity Columns; Takara  
455 Bio) and the target proteins were eluted according to the manufacturer's instructions. The  
456 desalted His-SUMO-YjbI(Y63F) and His-SUMO-TasA<sub>28-261</sub> were then treated with SUMO  
457 protease (SUMO protease; Sigma-Aldrich) and passed through the column again to obtain  
458 untagged Y63F and TasA<sub>28-261</sub> derivatives from the wash fraction, respectively.

459 TasA<sub>28-261</sub>-His, a mature form of TasA (Diehl et al., 2018) (amino acid residues 28-  
460 261) with a His-tag at the C-terminus was produced in *E. coli* BL21(DE3)/pEtasA2

(Supplementary File 1) by culturing the cells in LB medium at 37 °C for 6 h, followed by induction with 25 µM isopropyl β-D-1-thiogalactopyranoside and further cultivation for 10 h. The cells were harvested by centrifugation and lysed in B-PER (Thermo Fisher Scientific) supplemented with approximately 1 mM PMSF. The crude extract was applied onto a nickel chelation column (His GraviTrap, GE Healthcare), and TasA<sub>28-261</sub>-His was eluted according to the manufacturer's instructions.

#### ***In vitro* ROS-induced TasA aggregation**

Purified TasA<sub>28-261</sub>-His (200 µg) was incubated with 1 mM hydrogen peroxide and 10 µM FeCl<sub>2</sub> in the presence or absence of Yjbl (15 µg) in 50 mM Tris-acetate buffer (pH 7.4) at 37 °C for 30 min. The proteins, after being precipitated by adding four volumes of cold acetone, were harvested by centrifugation, and dissolved in a standard SDS sample buffer (0.125 M Tris (pH 6.8), 10% (w/w) 2-mercaptoethanol, 4% (w/w) SDS, 10% (w/w) sucrose, 0.01% (w/w) bromophenol blue), which was followed by SDS-PAGE and western blot analysis of TasA<sub>28-261</sub>-His with an anti-His-tag antibody.

#### **Analysis of Yjbl cell-surface localisation following extracellular protease digestion**

Yjbl cell-surface localisation was analysed following extracellular protease digestion of an intact *B. subtilis* pellicle. *B. subtilis* pellicle (10 mg) was incubated in 50 mM Tris-acetate buffer (pH 7.4) containing 5 mg/mL protease mixture (Pronase E, Sigma-Aldrich) in a total volume of 1 mL at 28 °C for 2 h and then directly resuspended in the standard SDS sample buffer before SDS-PAGE and western blot analysis.

#### **SDS-PAGE and western blot analysis**



Lysates in the standard SDS sample buffer were heated and then resolved on a 4–20% SDS/PAGE gradient gel (Mini-PROTEAN, Bio-Rad), followed by electroblotting on a PVDF membrane via a Trans Blot Turbo (Bio-Rad) at 25 V for 30 min. The membrane was blocked with 1% (w/w) skim milk in TBS (50 mM Tris-HCl and 0.85% (w/w) NaCl, pH 7.4) at 37 °C for 1 h, incubated with an anti-YjbI or anti-His-tag antibody at a dilution of 1: 1000 (vol/vol) in 37 °C TBS for 2 h, washed in TBST (TBS with 0.1% (v/v) Tween-20), and then incubated with a secondary goat anti-rabbit (for the anti-YjbI antiserum) or goat anti-mouse (for the anti-His-tag antibody) antibody conjugated with horseradish peroxidase (Bio-Rad) for 2 h. After the membrane was washed in TBST, the immunoreactive bands were visualised using 1-Step Ultra TMB (Pierce). The membrane was photographed using a gel imager (Gel Doc, Bio-Rad).

The anti-His-tag monoclonal antibody was purchased from Medical and Biological Laboratories (Nagoya, Japan), and the anti-YjbI antiserum was a rabbit serum purchased from Sigma Genosys. The anti-YjbI antiserum was prepared by immunising rabbits with purified YjbI mixed with complete Freund's adjuvant, boosting five times with each a week apart.

#### **Planktonically grown *B. subtilis* strains under AAPH-induced oxidative stress**

After growth in LB medium at 37 °C for 8 h, a 3-μL aliquot of the *B. subtilis* culture was inoculated (at OD<sub>600</sub> = 0.02) into 5 mL LB liquid medium containing 0, 25, 50, or 100 mM AAPH at 37 °C for 31 h. A small amount of each culture was fractionated at 0, 2, 4, 6, 8, 10, 12, 15, 20, 25, and 31 h. Next, each fractionated culture was diluted with 0.9% (w/w) saline to keep the absorbance ≤ 1.0 and then measured at 600 nm.

#### **Minimum bactericidal concentration assay for hypochlorous acid**

Pre-cultured *B. subtilis* strains (50  $\mu$ L) were mixed with 950  $\mu$ L of phosphate-buffered saline (137 mM NaCl, 8.1 mM Na<sub>2</sub>HPO<sub>4</sub>, 2.68 mM KCl, and 1.47 mM KH<sub>2</sub>PO<sub>4</sub>, pH 7.4) containing HClO at final concentrations between 0 and 500 mM. After incubation at 37 °C for 1 h, a 10- $\mu$ L aliquot from each mixture was spread on LB solid medium. The cells were grown at 37 °C for 48 h before bacterial colony counting. Then, the minimum concentration of HClO that generated no colony was determined. Tetracycline was not added to the pre-culture and evaluation solid media in the *yjbI*/*yjbI*<sup>WT</sup> and point-mutated strains to ensure that tetracycline did not cause oxidative damage synergistically with HClO.

### **Generation of protein hydroperoxides**

BSA-OOH was generated by the Fenton reaction or oxidation with AAPH (Gieseg et al., 2000). For the Fenton reaction, 0.2 mg/mL BSA (fatty-acid-free, Sigma-Aldrich) was incubated with 150 mM hydrogen peroxide and 1 mM FeCl<sub>2</sub> in 150 mM acetate buffer (pH 5.0) in a total volume of 30  $\mu$ L at 37 °C for 15 min. To remove excess hydrogen peroxide and iron, 1 mL of 80% cold acetone was added and the sample was centrifuged at 20,000  $\times$  g for 10 min to precipitate BSA-OOH. For oxidation with AAPH, 0.2 mg/mL BSA or TasA was incubated with 25 mM AAPH in 50 mM tris-acetate buffer (pH 7.0) in a total volume of 30  $\mu$ L at 37 °C for 12 h. The reaction was terminated by adding 4 volumes of cold acetone. After centrifugation, precipitated BSA-OOH or TasA-OOH was recovered.

### **Analysis of the *YjbI*-mediated prevention of ROS-induced protein aggregation**

The effect of YjbI on ROS-induced BSA aggregation was examined in two experiments: a two-step reaction and a one-pot reaction. In the two-step reaction, BSA-OOH was prepared beforehand as described above and then incubated with 0.1 mg/mL YjbI in 50 mM Tris-acetate buffer (pH 7.0) at 37 °C for 3 h in a total volume of 15  $\mu$ L. In the one-pot reaction,

each 0.1 mg/mL globins (Yjbl, Hb, or Mb) and 25 mM AAPH was simultaneously added to 0.2 mg/mL BSA in 50 mM Tris-acetate buffer (pH 7.0) in a total volume of 30  $\mu$ L and incubated at 37 °C for 3 h. For both experiments, the reaction was stopped by adding 4 volumes of ice-cold acetone, and the precipitated proteins were recovered by centrifugation. Proteins were resolved by SDS-PAGE and visualized by silver staining (Wako, Silver Stain II Kit).

#### **Determination of the hydroperoxide groups in BSA**

After hydroperoxidation, the acetone-precipitated BSA was dissolved in 25 mM H<sub>2</sub>SO<sub>4</sub> to assess for the hydroperoxide groups on the protein, as described (Gieseg et al., 2000). In brief, nine volumes of dissolved BSA-OOH or TasA-OOH were mixed with one volume of 5 mM ferrous ammonium sulphate and 5 mM xylene orange in 25 mM H<sub>2</sub>SO<sub>4</sub> and incubated at 28 °C for 30 min in the dark. The  $A_{560}$  of the mixture was measured using a UV-Vis spectrophotometer (SH-9000, Corona Electric). The molar extinction coefficient of the xylene orange-Fe<sup>3+</sup> complex ( $1.5 \times 10^4 \text{ M}^{-1}\text{cm}^{-1}$ ) (Gieseg et al., 2000) in 25 mM H<sub>2</sub>SO<sub>4</sub> at 28 °C was used to determine the hydroperoxide concentration. The number of hydroperoxide residues per BSA subunit or mature TasA molecule (amino acids 28-261) was determined by calculating the mole of peroxide generated per mole of added BSA (molecular weight: 66,463) or mature TasA (molecular weight: 25,716).

**Statistical analyses.** Statistical differences between two experimental groups were identified using one-tailed Student's *t*-test assuming equal variance (Microsoft Excel for Mac v.16.16.21). No data points were removed from the data set before the analyses.

#### **Acknowledgements**

The authors thank K. Kitayama and T. Kurihara for help with amino acid sequence analysis. The gene-disrupted strains used in this research were provided by the National BioResource Project (NBRP), Japan. This work was supported by JSPS KAKENHI grant numbers JP18K14383 and JP20K15446, by the Program for the Third-Phase R-GIRO Research from Ritsumeikan University, and by a grant from the Japan Foundation for Applied Enzymology.

### Competing interests

The authors declare no competing financial interest.

### References

- ARNAOUTELI, S., BAMFORD, C. N., STANLEY-WALL & KOVACS T. A. 2021. *Bacillus subtilis* biofilm formation and social interactions. *Nat Rev Microbiol*, 19, 600-614. DOI: <https://doi.org/10.1038/s41579-021-00540-9>.
- ARNAOUTELI, S., FERREIRA, A. S., SCHOR, M., MORRIS, R. J., BROMLEY, K. M., JO, J., CORTEZ, K. L., SUKHODUB, T., PRESCOTT, A. R., DIETRICH, L. E. P., MACPHEE, C. E. & STANLEY-WALL, N. R. 2017. Bifunctionality of a biofilm matrix protein controlled by redox state. *Proc Natl Acad Sci U S A*, 114, E6184-E6191. DOI: <https://doi.org/10.1073/pnas.1707687114>
- ARNAOUTELI, S., MACPHEE, C. E. & STANLEY-WALL, N. R. 2016. Just in case it rains: building a hydrophobic biofilm the *Bacillus subtilis* way. *Curr Opin Microbiol*, 34, 7-12. DOI: <https://doi.org/10.1016/j.mib.2016.07.012>
- ARYA, S., SETHI, D., SINGH, S., HADE, M. D., SINGH, V., RAJU, P., CHODISETTI, S. B., VERMA, D., VARSHNEY, G. C., AGREWALA, J. N. & DIKSHIT, K. L. 2013. Truncated hemoglobin, HbN, is post-translationally modified in *Mycobacterium tuberculosis* and modulates host-pathogen interactions during intracellular infection. *J Biol Chem*, 288, 29987-99. DOI: <https://doi.org/10.1074/jbc.M113.507301>

588 ASCENZI, P., DE MARINIS, E., COLETTA, M. & VISCA, P. 2008. H<sub>2</sub>O<sub>2</sub> and NO scavenging by  
 589 *Mycobacterium leprae* truncated hemoglobin O. *Biochem Biophys Res Commun*, 373, 197-201. DOI:  
 590 <https://doi.org/10.1016/j.bbrc.2008.05.168>  
 591 AWAD, W., AL-ERYANI, Y., EKSTROM, S., LOGAN, D. T. & VON WACHENFELDT, C. 2019. Structural  
 592 basis for YjbH adaptor-mediated recognition of transcription factor Spx. *Structure*, 27, 923-936 e6.  
 593 DOI: <https://doi.org/10.1016/j.str.2019.03.009>  
 594 BABIOR, B. M. 1984. The respiratory burst of phagocytes. *J Clin Invest*, 73, 599-601. DOI:  
 595 <https://doi.org/10.1172/JCI111249>  
 596 BELOIN, C., VALLE, J., LATOUR-LAMBERT, P., FAURE, P., KZREMINSKI, M., BALESTRINO, D.,  
 597 HAAGENSEN, J. A., MOLIN, S., PRENSIER, G., ARBEILLE, B. & GHIGO, J. M. 2004. Global  
 598 impact of mature biofilm lifestyle on *Escherichia coli* K-12 gene expression. *Mol Microbiol*, 51, 659-  
 599 74. DOI: <https://doi.org/10.1046/j.1365-2958.2003.03865.x>  
 600 BOECHI, L., MANEZ, P. A., LUQUE, F. J., MARTI, M. A. & ESTRIN, D. A. 2010. Unraveling the molecular  
 601 basis for ligand binding in truncated hemoglobins: the trHbO *Bacillus subtilis* case. *Proteins*, 78, 962-  
 602 70. DOI: <https://doi.org/10.1002/prot.22620>  
 603 BRODEN, N. J., FLURY, S., KING, A. N., SCHROEDER, B. W., COE, G. D. & FAULKNER, M. J. 2016.  
 604 Insights into the function of a second, nonclassical Ahp peroxidase, AhpA, in oxidative stress  
 605 resistance in *Bacillus subtilis*. *J Bacteriol*, 198, 1044-57. DOI: <https://doi.org/10.1128/JB.00679-15>  
 606 BUCHER, T., KARTVELISHVILI, E. & KOLODKIN-GAL, I. 2016. Methodologies for studying *B. subtilis*  
 607 biofilms as a model for characterizing small molecule biofilm inhibitors. *J Vis Exp*. DOI:  
 608 <https://doi.org/10.3791/5461>  
 609 BUSTAMANTE, J. P., RADUSKY, L., BOECHI, L., ESTRIN, D. A., TEN HAVE, A. & MARTI, M. A. 2016.  
 610 Evolutionary and functional relationships in the truncated hemoglobin family. *PLoS Comput Biol*, 12,  
 611 e1004701. DOI: <https://doi.org/10.1371/journal.pcbi.1004701>  
 612 CABISCOL, E., TAMARIT, J. & ROS, J. 2000. Oxidative stress in bacteria and protein damage by reactive  
 613 oxygen species. *Int Microbiol*, 3, 3-8.  
 614 CANDEIAS, L. P., PATEL, K. B., STRATFORD, M. R. & WARDMAN, P. 1993. Free hydroxyl radicals are  
 615 formed on reaction between the neutrophil-derived species superoxide anion and hypochlorous acid.  
 616 *FEBS Lett*, 333, 151-3. DOI: [https://doi.org/10.1016/0014-5793\(93\)80394-a](https://doi.org/10.1016/0014-5793(93)80394-a)  
 617 CANDEIAS, L. P., STRATFORD, M. R. & WARDMAN, P. 1994. Formation of hydroxyl radicals on reaction

618 of hypochlorous acid with ferrocyanide, a model iron(II) complex. *Free Radic Res*, 20, 241-9. DOI:  
619 <https://doi.org/10.3109/10715769409147520>

620 CHEN, L., KERAMATI, L. & HELMANN, J. D. 1995. Coordinate regulation of *Bacillus subtilis* peroxide  
621 stress genes by hydrogen peroxide and metal ions. *Proc Natl Acad Sci U S A*, 92, 8190-4. DOI:  
622 <https://doi.org/10.1073/pnas.92.18.8190>

623 CHOUDHARY, M. L., JAWAID, S., AHUJA, M. K., SHIVA, N. K., GUPTA, P., BHUYAN, A. K. & KHATRI,  
624 G. S. 2005. Open reading frame *yjbl* of *Bacillus subtilis* codes for truncated hemoglobin. *Protein Expr*  
625 *Purif*, 41, 363-72. DOI: <https://doi.org/10.1016/j.pep.2005.02.022>

626 COUTURE, M., YEH, S. R., WITTENBERG, B. A., WITTENBERG, J. B., OUELLET, Y., ROUSSEAU, D. L.  
627 & GUERTIN, M. 1999. A cooperative oxygen-binding hemoglobin from *Mycobacterium tuberculosis*.  
628 *Proc Natl Acad Sci U S A*, 96, 11223-8. DOI: <https://doi.org/10.1073/pnas.96.20.11223>, PMID: 18015

629 DAVIES, M. J. 2016. Protein oxidation and peroxidation. *Biochem J*, 473, 805-25. DOI:  
630 <https://doi.org/10.1042/BJ20151227>

631 DAVIES, M. J., FU, S. & DEAN, R. T. 1995. Protein hydroperoxides can give rise to reactive free radicals.  
632 *Biochem J*, 305 ( Pt 2), 643-9. DOI: <https://doi.org/10.1042/bj3050643>

633 DEAN, R. T., FU, S., STOCKER, R. & DAVIES, M. J. 1997. Biochemistry and pathology of radical-mediated  
634 protein oxidation. *Biochem J*, 324 ( Pt 1), 1-18.

635 DIEHL, A., ROSKE, Y., BALL, L., CHOWDHURY, A., HILLER, M., MOLIERE, N., KRAMER, R.,  
636 STOPPLER, D., WORTH, C. L., SCHLEGEL, B., LEIDERT, M., CREMER, N., ERDMANN, N.,  
637 LOPEZ, D., STEPHANOWITZ, H., KRAUSE, E., VAN ROSSUM, B. J., SCHMIEDER, P.,  
638 HEINEMANN, U., TURGAY, K., AKBEY, U. & OSCHKINAT, H. 2018. Structural changes of TasA  
639 in biofilm formation of *Bacillus subtilis*. *Proc Natl Acad Sci U S A*, 115, 3237-3242. DOI:  
640 <https://doi.org/10.1073/pnas.1718102115>

641 ERSKINE, S., MORRIS, J. R., SCHOR, M., EARL, C., GILLESPIE, C. M. R., BROMLEY, M. K.,  
642 SUKHODUB, T., CLARK, L., FYFE, K. P., SERPELL, C. L., STANLEY-WALL & MACPHEE, E. C.  
643 2018. Formation of functional, non-amyloidogenic fibres by recombinant *Bacillus subtilis* TasA. *Mol*  
644 *Microbiol*, 110, 897-913. DOI: <https://doi.org/10.1111/mmi.13985>

645 EZRATY, B., GENNARIS, A., BARRAS, F. & COLLET, J. F. 2017. Oxidative stress, protein damage and  
646 repair in bacteria. *Nat Rev Microbiol*, 15, 385-396. DOI: <https://doi.org/10.1038/nrmicro.2017.26>

647 FABIANEK, R. A., HENNECKE, H. & THONY-MEYER, L. 2000. Periplasmic protein thiol:disulfide

648 oxidoreductases of *Escherichia coli*. *FEMS Microbiol Rev*, 24, 303-16. DOI:  
 649 <https://doi.org/10.1111/j.1574-6976.2000.tb00544.x>  
 650 FANG, Z. & DOS SANTOS, P. C. 2015. Protective role of bacillithiol in superoxide stress and Fe-S metabolism  
 651 in *Bacillus subtilis*. *Microbiologyopen*, 4, 616-31. DOI: <https://doi.org/10.1002/mbo3.267>  
 652 FEIS, A., LAPINI, A., CATACCHIO, B., BROGIONI, S., FOGGI, P., CHIANCONE, E., BOFFI, A. &  
 653 SMULEVICH, G. 2008. Unusually strong H-bonding to the heme ligand and fast geminate  
 654 recombination dynamics of the carbon monoxide complex of *Bacillus subtilis* truncated hemoglobin.  
 655 *Biochemistry*, 47, 902-10. DOI: <https://doi.org/10.1021/bi701297f>  
 656 FUANGTHONG, M., ATICHARTPONGKUL, S., MONGKOLSUK, S. & HELMANN, J. D. 2001. OhrR is a  
 657 repressor of *ohrA*, a key organic hydroperoxide resistance determinant in *Bacillus subtilis*. *J Bacteriol*,  
 658 183, 4134-41. DOI: <https://doi.org/10.1128/JB.183.14.4134-4141.2001>  
 659 GABALLA, A., NEWTON, G. L., ANTELMANN, H., PARSONAGE, D., UPTON, H., RAWAT, M.,  
 660 CLAIBORNE, A., FAHEY, R. C. & HELMANN, J. D. 2010. Biosynthesis and functions of bacillithiol,  
 661 a major low-molecular-weight thiol in *Bacilli*. *Proc Natl Acad Sci U S A*, 107, 6482-6. DOI:  
 662 <https://doi.org/10.1073/pnas.100092810>  
 663 GALARIS, D., CADENAS, E. & HOCHSTEIN, P. 1989. Glutathione-dependent reduction of peroxides during  
 664 ferryl- and met-myoglobin interconversion: a potential protective mechanism in muscle. *Free Radic*  
 665 *Biol Med*, 6, 473-8. DOI: [https://doi.org/10.1016/0891-5849\(89\)90039-7](https://doi.org/10.1016/0891-5849(89)90039-7)  
 666 GEBICKI, J. M. 1997. Protein hydroperoxides as new reactive oxygen species. *Redox Rep*, 3, 99-110. DOI:  
 667 <https://doi.org/10.1080/13510002.1997.11747096>  
 668 GEBICKI, S. & GEBICKI, J. M. 1993. Formation of peroxides in amino acids and proteins exposed to oxygen  
 669 free radicals. *Biochem J*, 289 ( Pt 3), 743-9.  
 670 GEBICKI, S. & GEBICKI, J. M. 1999. Crosslinking of DNA and proteins induced by protein hydroperoxides.  
 671 *Biochem J*, 338 ( Pt 3), 629-36.  
 672 GEBICKI, S., GILL, K. H., DEAN, R. T. & GEBICKI, J. M. 2002. Action of peroxidases on protein  
 673 hydroperoxides. *Redox Rep*, 7, 235-42. DOI: <https://doi.org/10.1179/135100002125000541>  
 674 GIANGIACOMO, L., ILARI, A., BOFFI, A., MOREA, V. & CHIANCONE, E. 2005. The truncated oxygen-  
 675 avid hemoglobin from *Bacillus subtilis*: X-ray structure and ligand binding properties. *J Biol Chem*,  
 676 280, 9192-202. DOI: <https://doi.org/10.1074/jbc.M407267200>  
 677 GIESEG, S., DUGGAN, S. & GEBICKI, J. M. 2000. Peroxidation of proteins before lipids in U937 cells

678 exposed to peroxy radicals. *Biochem J*, 350 Pt 1, 215-8.

679 GIULIVI, C. & DAVIES, K. J. 2001. Mechanism of the formation and proteolytic release of H<sub>2</sub>O<sub>2</sub>-induced  
680 dityrosine and tyrosine oxidation products in hemoglobin and red blood cells. *J Biol Chem*, 276,  
681 24129-36. DOI: <https://doi.org/10.1074/jbc.M010697200>

682 GUDDAT, L. W., BARDWELL, J. C. & MARTIN, J. L. 1998. Crystal structures of reduced and oxidized DsbA:  
683 investigation of domain motion and thiolate stabilization. *Structure*, 6, 757-67. DOI:  
684 [https://doi.org/10.1016/s0969-2126\(98\)00077-x](https://doi.org/10.1016/s0969-2126(98)00077-x)

685 HADE, M. D., SETHI, D., DATTA, H., SINGH, S., THAKUR, N., CHHAYA, A. & DIKSHIT, K. L. 2020.  
686 Truncated hemoglobin O carries an autokinase activity and facilitates adaptation of *mycobacterium*  
687 *tuberculosis* under hypoxia. *Antioxid Redox Signal*, 32, 351-362. DOI:  
688 <https://doi.org/10.1089/ars.2018.7708>

689 HALL, C. W. & MAH, T. F. 2017. Molecular mechanisms of biofilm-based antibiotic resistance and tolerance in  
690 pathogenic bacteria. *FEMS Microbiol Rev*, 41, 276-301. DOI: <https://doi.org/10.1093/femsre/fux010>

691 HARWOOD, C. R. & CUTTING, S. M. 1990. *Molecular biological methods for Bacillus*, Chichester ; New  
692 York, Wiley.

693 HAWKINS, C. L. & DAVIES, M. J. 1998. Hypochlorite-induced damage to proteins: formation of nitrogen-  
694 centred radicals from lysine residues and their role in protein fragmentation. *Biochem J*, 332 ( Pt 3),  
695 617-25. DOI: <https://doi.org/10.1042/bj3320617>

696 HAYASHI, T., HITOMI, Y., ANDO, T., MIZUTANI, T., HISAEDA, Y., KITAGAWA. & OGOSHI, H. 1999.  
697 Peroxidase activity of myoglobin is enhanced by chemical mutation of heme-propionates. *J Am Chem*  
698 *Soc*, 121,7747-7750. DOI: <https://doi.org/10.1021/ja9841005>

699 HEINECKE, J. W., LI, W., DAEHNKE, H. L., 3RD & GOLDSTEIN, J. A. 1993. Dityrosine, a specific marker  
700 of oxidation, is synthesized by the myeloperoxidase-hydrogen peroxide system of human neutrophils  
701 and macrophages. *J Biol Chem*, 268, 4069-77.

702 HOBLEY, L., HARKINS, C., MACPHEE, C. E. & STANLEY-WALL, N. R. 2015. Giving structure to the  
703 biofilm matrix: an overview of individual strategies and emerging common themes. *FEMS Microbiol*  
704 *Rev*, 39, 649-69. DOI: <https://doi.org/10.1093/femsre/fuv015>

705 KOBAYASHI, K. & IWANO, M. 2012. BslA(YuaB) forms a hydrophobic layer on the surface of *Bacillus*  
706 *subtilis* biofilms. *Mol Microbiol*, 85, 51-66. DOI: <https://doi.org/10.1111/j.1365-2958.2012.08094.x>

707 KOROVILA, I., HUGO, M., CASTRO, J. P., WEBER, D., HOHN, A., GRUNE, T. & JUNG, T. 2017.



708 Proteostasis, oxidative stress and aging. *Redox Biol*, 13, 550-567. DOI:  
709 <https://doi.org/10.1016/j.redox.2017.07.008>

710 LAPINI, A., DI DONATO, M., PATRIZI, B., MARCELLI, A., LIMA, M., RIGHINI, R., FOGGI, P.,  
711 SCIAMANNA, N. & BOFFI, A. 2012. Carbon monoxide recombination dynamics in truncated  
712 hemoglobins studied with visible-pump MidIR-probe spectroscopy. *J Phys Chem B*, 116, 8753-61.  
713 DOI: <https://doi.org/10.1021/jp3019149>

714 LARSSON, J. T., ROGSTAM, A. & VON WACHENFELDT, C. 2007. YjbH is a novel negative effector of the  
715 disulphide stress regulator, Spx, in *Bacillus subtilis*. *Mol Microbiol*, 66, 669-84. DOI:  
716 <https://doi.org/10.1111/j.1365-2958.2007.05949.x>

717 LING, J., CHO, C., GUO, L. T., AERNI, H. R., RINEHART, J. & SOLL, D. 2012. Protein aggregation caused  
718 by aminoglycoside action is prevented by a hydrogen peroxide scavenger. *Mol Cell*, 48, 713-22. DOI:  
719 <https://doi.org/10.1016/j.molcel.2012.10.001>

720 LIU, C., HE, Y. & CHANG, Z. 2004. Truncated hemoglobin o of *Mycobacterium tuberculosis*: the oligomeric  
721 state change and the interaction with membrane components. *Biochem Biophys Res Commun*, 316,  
722 1163-72. DOI: <https://doi.org/10.1016/j.bbrc.2004.02.170>

723 MANCA, C., PAUL, S., BARRY, C. E., 3RD, FREEDMAN, V. H. & KAPLAN, G. 1999. *Mycobacterium*  
724 *tuberculosis* catalase and peroxidase activities and resistance to oxidative killing in human monocytes  
725 in vitro. *Infect Immun*, 67, 74-9.

726 MASKOS, Z., RUSH, J. D. & KOPPENOL, W. H. 1992. The hydroxylation of phenylalanine and tyrosine: a  
727 comparison with salicylate and tryptophan. *Arch Biochem Biophys*, 296, 521-9. DOI:  
728 [https://doi.org/10.1016/0003-9861\(92\)90606-w](https://doi.org/10.1016/0003-9861(92)90606-w)

729 MIELICH-SUSS & LOPEZ, D. 2014. Molecular mechanisms involved in *Bacillus subtilis* biofilm formation.  
730 *Environ Microbiol*, 17, 555-65. DOI: <https://doi.org/10.1111/1462-2920.12527>

731 MORGAN, P. E., DEAN, R. T. & DAVIES, M. J. 2004. Protective mechanisms against peptide and protein  
732 peroxides generated by singlet oxygen. *Free Radic Biol Med*, 36, 484-96. DOI:  
733 <https://doi.org/10.1016/j.freeradbiomed.2003.11.021>

734 NICOLETTI, F. P., COMANDINI, A., BONAMORE, A., BOECHI, L., BOUBETA, F. M., FEIS, A.,  
735 SMULEVICH, G. & BOFFI, A. 2010. Sulfide binding properties of truncated hemoglobins.  
736 *Biochemistry*, 49, 2269-78. DOI: <https://doi.org/10.1021/bi901671d>

737 OUELLET, H., JUSZCZAK, L., DANTSKER, D., SAMUNI, U., OUELLET, Y. H., SAVARD, P. Y.,

738 WITTENBERG, J. B., WITTENBERG, B. A., FRIEDMAN, J. M. & GUERTIN, M. 2003. Reactions  
739 of *Mycobacterium tuberculosis* truncated hemoglobin O with ligands reveal a novel ligand-inclusive  
740 hydrogen bond network. *Biochemistry*, 42, 5764-74. DOI: <https://doi.org/10.1021/bi0270337>

741 OUELLET, H., OUELLET, Y., RICHARD, C., LABARRE, M., WITTENBERG, B., WITTENBERG, J. &  
742 GUERTIN, M. 2002. Truncated hemoglobin HbN protects *Mycobacterium bovis* from nitric oxide.  
743 *Proc Natl Acad Sci U S A*, 99, 5902-7. DOI: <https://doi.org/10.1073/pnas.092017799>

744 OUELLET, H., RANGUELOVA, K., LABARRE, M., WITTENBERG, J. B., WITTENBERG, B. A.,  
745 MAGLIOZZO, R. S. & GUERTIN, M. 2007. Reaction of *Mycobacterium tuberculosis* truncated  
746 hemoglobin O with hydrogen peroxide: evidence for peroxidatic activity and formation of protein-  
747 based radicals. *J Biol Chem*, 282, 7491-503. DOI: <https://doi.org/10.1074/jbc.M609155200>

748 PAWARIA, S., RAJAMOHAN, G., GAMBHIR, V., LAMA, A., VARSHNEY, G. C. & DIKSHIT, K. L. 2007.  
749 Intracellular growth and survival of *Salmonella enterica* serovar *Typhimurium* carrying truncated  
750 hemoglobins of *Mycobacterium tuberculosis*. *Microb Pathog*, 42, 119-28. DOI:  
751 <https://doi.org/10.1016/j.micpath.2006.12.001>

752 PESKIN, V. A., COX, G. A., NAGY, P., MORGAN, E. P., HAMPTON, B. M., DAVIES, J. M. &  
753 WINTERBOURN, C. C. 2007. Removal of amino acid, peptide and protein hydroperoxides by reaction  
754 with peroxiredoxins 2 and 3. *Biochem J*, 432, 313-21. DOI: <https://doi.org/10.1042/BJ20101156>

755 RAHMANTO, S. A. & DAVIES, J. M. 2011. Catalytic activity of selenomethionine in removing amino acid,  
756 peptide, and protein hydroperoxides. *Free Radic Biol Med*, 51, 2288-99. DOI:  
757 <https://doi.org/10.1016/j.freeradbiomed.2011.09.027>

758 ROGSTAM, A., LARSBISON, J. T., KJELGAARD, P. & VON WACHENFELDT, C. 2007. Mechanisms of  
759 adaptation to nitrosative stress in *Bacillus subtilis*. *J Bacteriol*, 189, 3063-71. DOI:  
760 <https://doi.org/10.1128/JB.01782-06>

761 ROMERO, D., AGUILAR, C., LOSICK, R. & KOLTER, R. 2010. Amyloid fibers provide structural integrity to  
762 *Bacillus subtilis* biofilms. *Proc Natl Acad Sci U S A*, 107, 2230-4. DOI:  
763 <https://doi.org/10.1073/pnas.0910560107>

764 ROMERO, D., VLAMAKIS, H., LOSICK, R. & KOLTER, R. 2011. An accessory protein required for  
765 anchoring and assembly of amyloid fibres in *B. subtilis* biofilms. *Mol Microbiol*, 80, 1155-68. DOI:  
766 <https://doi.org/10.1111/j.1365-2958.2011.07653.x>

767 SALEH, M., BARTUAL, S. G., ABDULLAH, M. R., JENSCH, I., ASMAT, T. M., PETRUSCHKA, L.,

768           PRIBYL, T., GELLERT, M., LILLIG, C. H., ANTELMANN, H., HERMOSO, J. A. &  
 769           HAMMERSCHMIDT, S. 2013. Molecular architecture of *Streptococcus pneumoniae* surface  
 770           thioredoxin-fold lipoproteins crucial for extracellular oxidative stress resistance and maintenance of  
 771           virulence. *EMBO Mol Med*, 5, 1852-70. DOI: <https://doi.org/10.1002/emmm.201202435>  
 772           STADTMAN, E. R. & LEVINE, R. L. 2003. Free radical-mediated oxidation of free amino acids and amino  
 773           acid residues in proteins. *Amino Acids*, 25, 207-18. DOI: <https://doi.org/10.1007/s00726-003-0011-2>  
 774           STUDIER, F. W. & MOFFATT, B. A. 1986. Use of bacteriophage T7 RNA polymerase to direct selective high-  
 775           level expression of cloned genes. *J Mol Biol*, 189, 113-30.  
 776           SVISTUNENKO, D. A. 2005. Reaction of haem containing proteins and enzymes with hydroperoxides: the  
 777           radical view. *Biochim Biophys Acta*, 1707, 127-55. DOI: <https://doi.org/10.1016/j.bbabi.2005.01.004>  
 778           TORGE, R., COMANDINI, A., CATACCHIO, B., BONAMORE, A., BOTTA, B. & BOFFI, A. 2009.  
 779           Peroxidase-like activity of *Thermobifida fusca* hemoglobin: The oxidation of dibenzylbutanolide. *J*  
 780           *Mol Catal B Enzym*, 61, 303-308.  
 781           VLAMAKIS, H., AGUILAR, C., LOSICK, R. & KOLTER, R. 2008. Control of cell fate by the formation of an  
 782           architecturally complex bacterial community. *Genes Dev*, 22, 945-53. DOI: [https://doi.org/](https://doi.org/10.1101/gad.1645008)  
 783           10.1101/gad.1645008.  
 784           VULETICH, D. A. & LECOMTE, J. T. 2006. A phylogenetic and structural analysis of truncated hemoglobins.  
 785           *J Mol Evol*, 62, 196-210. DOI: <https://doi.org/10.1007/s00239-005-0077-4>  
 786           WANG, Y., BARBEAU, X., BILIMORIA, A., LAGUE, P., COUTURE, M. & TANG, J. K. 2015. Peroxidase  
 787           activity and involvement in the oxidative stress response of *Roseobacter denitrificans* truncated  
 788           hemoglobin. *PLoS One*, 10, e0117768. DOI: <https://doi.org/10.1371/journal.pone.0117768>  
 789           WELCH, K. D., DAVIS, T. Z., VAN EDEN, M. E. & AUST, S. D. 2002. Deleterious iron-mediated oxidation of  
 790           biomolecules. *Free Radic Biol Med*, 32, 577-83. DOI: [https://doi.org/10.1016/s0891-5849\(02\)00760-8](https://doi.org/10.1016/s0891-5849(02)00760-8)  
 791           WITTENBERG, J. B., BOLOGNESI, M., WITTENBERG, B. A. & GUERTIN, M. 2002. Truncated  
 792           hemoglobins: a new family of hemoglobins widely distributed in bacteria, unicellular eukaryotes, and  
 793           plants. *J Biol Chem*, 277, 871-4. DOI: <https://doi.org/10.1074/jbc.R100058200>  
 794           ZEIGLER, R. D., PRAGAI, Z., RODRIGUEZ, S., CHEVREUX, B., MUFFLER, A., ALBERT, T., BAI, R.,  
 795           WYSS, M. & PERKINS, B. J. 2008. The origins of 168, W23, and other *Bacillus subtilis* legacy  
 796           strains. *J Bacteriol*, 190, 6983-95. DOI: <https://doi.org/10.1128/JB.00722-08>

797



## Figure legend

**Fig. 1.** YjbI is needed for normal biofilm formation. Images showing the morphology (left panels) and surface repellency (right panels) of the biofilms of the WT, *yjbI*, *yjbI/yjbI<sup>WT</sup>*, and *tasA*-deficient (*tasA<sup>-</sup>*) strains of *B. subtilis*. The water contact angles indicated in the right panels represent the mean  $\pm$  SD of three independent experiments (n = 3).

**Fig. 2.** *yjbI* is required to prevent oxidative TasA aggregation and for the normal antioxidant properties of *B. subtilis* cells. (a) Detection of His-tagged TasA (TasA-His) in the soluble (left panel) and insoluble (right panel) fractions of the pellicles of the WT strain or *yjbI*-deficient mutant (*yjbI*) strain carrying p<sub>HtasA1</sub>, which constitutively expresses TasA-His (Supplementary File 1). After culturing in liquid MSgg medium, lysates of these pellicles were further analysed by western blotting using an anti-His-tag antibody. The positions of the molecular mass marker proteins are shown on the left. The arrowheads and bracket indicate monomeric and aggregated TasA-His, respectively. Similar results were obtained from three independent experiments. (b) *In vitro* ROS-induced formation of aggregates of purified TasA (p<sub>EtasA2</sub>-derived TasA<sub>28-261</sub>-His) (Supplementary File 1) in the presence (+) or absence (-) of purified recombinant YjbI, as evidenced by western blotting analysis using an anti-His-tag antibody. The arrowhead and bracket indicate monomeric and aggregated TasA<sub>28-261</sub>-His, respectively. Protein aggregation was induced with 1 mM H<sub>2</sub>O<sub>2</sub> and 10  $\mu$ M FeCl<sub>2</sub>. Similar results were obtained from two independent experiments. (c) Localisation of YjbI in the insoluble biofilm fraction. The soluble and insoluble fractions of the WT and *yjbI* pellicles and culture supernatants (sup) were analysed by western blotting using an anti-YjbI antiserum. Similar results were obtained from two independent experiments. (d) Localisation of YjbI to the cell surface, as evidenced by western blot analysis of the intact WT pellicles with (+) or without (-) protease digestion. YjbI was detected using an anti-YjbI antiserum.

Similar results were obtained from two independent experiments. (e) Images showing biofilm surface repellency. Two microliters of rabbit anti-YjbI serum (left panel) or pre-immune serum (right panel) were mixed with 2  $\mu$ L of pre-cultured *B. subtilis* cells and inoculated on MSgg solid medium. The morphologies of the biofilms are shown in the insets. The water contact angles indicated in the right panels represent the mean  $\pm$  SD of three independent experiments. (f) Sensitivity of planktonically grown *B. subtilis* strains to AAPH-induced oxidative stress. *B. subtilis* cells (WT, *yjbI*<sup>-</sup>, *tasA*<sup>-</sup>, or *yjbH*<sup>-</sup>) were inoculated at OD<sub>600</sub> = 0.02 in LB medium containing 0–100 mM AAPH and grown at 37°C with shaking. Data are shown as the mean  $\pm$  SD of three independent experiments.

**Fig. 3.** YjbI exhibits protein hydroperoxide peroxidase activity. (a) Schematic drawing summarising the proposed protein cross-linking and fragmentation induced by protein radicals derived from protein hydroperoxides and prevention of these reactions by the protein hydroperoxide peroxidase activity of YjbI. The solid and dashed arrows indicate the already known reactions (Davies, 2016) occurring at protein side chains and backbones, respectively. Protein cross-linking proceeds via spontaneous radical coupling (red arrows), and the Michael addition occurs at protein side chains (yellow arrow). YjbI catalyses the protein hydroperoxide peroxidase reaction (blue arrow) to convert protein hydroperoxides (ROOH) to hydroxy groups (ROH) at protein side chains and prevents further protein cross-linking and fragmentation. Side chain alkoxyl radicals (RO $\cdot$ ) can be formed through one-electron reduction (e.g. homolysis) of ROOH, followed by hydrogen atom abstraction reactions with other protein side chains or backbones (R'H). The carbon-centred radicals (R' $\cdot$ ) of side chains or backbones lead to protein cross-linking to yield protein aggregates (indicated with solid and dashed red arrows). The side chain or backbone R' $\cdot$  also reacts with oxygen to produce protein peroxy radicals (R'OO $\cdot$ ) under aerobic conditions. The side chain R'OO $\cdot$  reacts with

849 the side chains or backbones of other amino acid residues (RH) in its vicinity to yield protein  
 850 ROOH moieties. The unstable backbone  $R'OO\cdot$  and ROOH moieties cause protein  
 851 fragmentation. (b) BSA was treated with (+) or without (-)  $H_2O_2$  and  $FeCl_2$  to produce BSA-  
 852 OOH by Fenton reaction. BSA-OOH was incubated in the presence (+) or absence (-) of Yjbl  
 853 and analysed by SDS-PAGE and silver staining. Yjbl and monomeric BSA are indicated by  
 854 arrows, and BSA aggregates and fragments are indicated by brackets. The sizes of the  
 855 molecular mass marker proteins (M) are shown on the left. Similar results were obtained  
 856 from two independent experiments. (c) BSA-OOH prepared by AAPH treatment was  
 857 incubated in the presence (+) or absence (-) of Yjbl and analysed by SDS-PAGE and silver  
 858 staining. The labels on the left or right of the images are the same as those in (b). Similar  
 859 results were obtained from two independent experiments. (d) Yjbl prevents AAPH-induced  
 860 BSA-OOH aggregation. BSA was incubated for 3 h with (+) or without (-) AAPH before  
 861 adding Yjbl, haemoglobin from bovine blood (Hb) (Sigma-Aldrich), myoglobin from equine  
 862 heart (Mb) (Sigma-Aldrich), or none (-) and then analysed by SDS-PAGE and silver staining.  
 863 The positions of the molecular mass marker proteins (M) are shown on the left. Similar  
 864 results were obtained from two independent experiments. (e) Time course of the *Yjbl*-induced  
 865 reduction of the hydroperoxide groups in BSA-OOH. Peroxide-treated BSA (30  $\mu$ M) in 50  
 866 mM Tris-acetate buffer (pH 7.0) was incubated with (blue circles) or without (red circles)  
 867 Yjbl (3.3  $\mu$ M) at 37°C, and the reaction was terminated by adding 4 volumes of cold acetone  
 868 at the indicated incubation times (0, 0.5, 1, 2, 5, 7, and 20 min). The number of  
 869 hydroperoxide groups per BSA subunit was determined for each sample. The data are the  
 870 mean  $\pm$  SD of three independent experiments (\* $p$  < 0.05; \*\* $p$  < 0.01; and \*\*\* $p$  < 0.005; *t*-test,  
 871 one-tailed). (f) TasA-OOH (30  $\mu$ M) in 50 mM Tris-acetate buffer (pH 7.0) was incubated  
 872 with Yjbl (3.3  $\mu$ M) at 37°C, and the reaction was terminated by adding four volumes of cold  
 873 acetone after incubation for 20 min. The number of hydroperoxide groups per TasA was

determined for each sample. Data are shown as the mean  $\pm$  SD of three independent experiments (\*\* $p < 0.005$ ;  $t$ -test, one-tailed).

**Fig. 4.** Gene complementation study using the *yjbI*-deficient strain of *B. subtilis* with plasmids expressing YjbI derivatives (Y25F, Y63F, and W89F). (a) The morphology and surface repellence of the biofilms of the *yjbI*-deficient strains carrying each plasmid are shown. The water contact angles indicated in the right panels represent the mean  $\pm$  SD of three independent experiments ( $n = 3$ ). (b) BSA-OOH (30  $\mu$ M) in 50 mM Tris-acetate buffer (pH 7.0) was incubated with the YjbI derivative Y63F (3.3  $\mu$ M) at 37°C, and the reaction was terminated by adding four volumes of cold acetone after incubation for 20 min. The number of hydroperoxide groups per BSA subunit was determined for each sample. Data are shown as the mean  $\pm$  SD of three independent experiments.

**Fig. 5.** YjbI protects proteins and the cell from reactive oxygen species (ROS) by removing hydroperoxide groups from proteins. (a) YjbI repairs the oxidatively damaged TasA-OOH in biofilms. In the wild-type (WT) strain (left panel), the normal fibrous TasA (green trapezoids) is damaged by ROS to generate TasA-OOH (yellow trapezoid) on the cell surface. YjbI converts TasA-OOH to TasA-OH (blue trapezoid) to stabilise the normal TasA fibre. In contrast, TasA-OOH aggregates via radical-mediated protein cross-linking in the *yjbI*- strain (right panel). (b) A proposed role of YjbI in the general protection of cell-surface proteins from ROS-induced oxidative damage. Protein hydroperoxide-modified residues generated in various cellular surface proteins (red, green, and yellow ellipses) are generally reduced to protein hydroxy residues by YjbI to protect from further damage (i.e. aggregation) (left half). *yjbI* disruption accumulates protein aggregates via hydroperoxidation and cross-linking of various proteins, resulting in cell toxicity (right half).



**Table**

**Table 1.** Minimum bactericidal concentration following exposure to hypochlorous acid

(HClO) (n = 2)

(+) visible growth, (–) no visible growth

HClO (mM)	62.5	31.3	15.6	5.00	2.50	1.25	0.625	0.313	0.156
WT	–	+	+	+	+	+	+	+	+
<i>yjbI</i>	–	–	–	–	–	–	–	+	+

**Table 2.** Minimum bactericidal concentration following exposure to hypochlorous acid in the

*yjbI*/*yjbI*<sup>WT</sup> and point-mutated strains (HClO) (n = 2)

(+) visible growth, (–) no visible growth, (±) visible growth in one of two cases

HClO (mM)	62.5	31.3	15.6	5.00	2.50	1.25	0.625	0.313	0.156
<i>yjbI</i> / <i>yjbI</i> <sup>WT</sup>	–	–	–	–	–	+	+	+	+
<i>yjbI</i> / <i>yjbI</i> <sup>Y25F</sup>	–	–	–	–	–	–	–	+	+
<i>yjbI</i> / <i>yjbI</i> <sup>Y63F</sup>	–	–	–	–	–	–	–	+	+
<i>yjbI</i> / <i>yjbI</i> <sup>W89F</sup>	–	–	–	–	–	±	+	+	+

## 917    **Supplementary information**

918    **Figure 2-figure supplement 1.** Purification of YjbI. YjbI was produced in *E. coli*  
919    BL21(DE3)/pEyjbI2 cells grown in lysogeny broth (LB) medium. Proteins from each  
920    purification step (i.e., whole-cell and soluble crude extracts); 30–60% saturation ammonium  
921    sulphate (AS) fractionation; Sephacryl S-100 gel filtration; and Toyopearl DEAE-650M  
922    chromatography were resolved by SDS-PAGE and then stained with Coomassie Brilliant  
923    Blue.

924

925    **Figure 3-figure supplement 1.** Purification of TasA and YjbI (Y63F). Mature TasA was  
926    produced in *E. coli* BL21(DE3)/pEtasA3 cells grown in LB medium. Proteins from each  
927    purification step, i.e. soluble crude extracts (lane 1), elution fraction from immobilized metal  
928    affinity chromatography (IMAC) resin charged with cobalt (lane 2), and wash fraction from  
929    IMAC after treatment with SUMO-protease (lane 3), were resolved by SDS-PAGE and  
930    stained with Coomassie Brilliant Blue.

931

932    **Figure 3-figure supplement 2.** Lipid hydroperoxide (LOOH) levels were not affected in  
933    *yjbI*- strain biofilms. Bacterial colony biofilms were obtained by inoculating a 3- $\mu$ L aliquot of  
934    pre-cultured *B. subtilis* on solid MSgg medium, followed by cultivation at 37 °C for 48 h.  
935    The biofilms were collected and suspended in phosphate-buffered saline by using a spatula.  
936    These WT and *yjbI*-deficient mutant biofilm suspensions were analysed with a colorimetric  
937    LOOH assay kit (LPO assay kit, Cayman Chemical Company) according to the  
938    manufacturer's instructions. The data are shown as the mean  $\pm$  SD of three independent  
939    experiments ( $p = 0.083$ ;  $t$ -test, one-tailed).

940

941 **Figure 3-figure supplement 3.** X-ray crystal structure of *B. subtilis* Yjbl (PDB ID: 1UX8)  
 942 (Giangiacomo et al., 2005), showing an opening on the molecular surface. The protein  
 943 surface is shown in blue, and the haem molecule is shown with a stick model. The image was  
 944 drawn using PyMOL.

945

946 **Figure 4-figure supplement 1.** Y63F derivative of Yjbl was produced in *E. coli*  
 947 BL21(DE3)/pEyjbl3 cells grown in LB medium. Proteins from each purification step, soluble  
 948 crude extracts (lane 1), elution fraction from IMAC (lane 2), and wash fraction from IMAC  
 949 after treatment with SUMO-protease (lane 3) were resolved by SDS-PAGE and stained with  
 950 Coomassie Brilliant Blue. The positions of the molecular mass marker proteins (M) are  
 951 shown on the left.

952

953 **Figure 5-figure supplement 1.** *B. subtilis* Yjbl does not contain a predicted signal sequence.  
 954 The results of bioinformatic analyses by using PSORTb (<https://www.psort.org/psortb/>) or  
 955 SignalP-5.0 (<http://www.cbs.dtu.dk/services/SignalP/>).

956

## 957 **Strains and plasmids used in this study.**

Strain	Genotype	Source
<i>Bacillus subtilis</i> 168	<i>trpC2</i>	NBRP* <sup>1</sup>
BFS2846	<i>B. subtilis</i> 168 <i>yjbl::erm</i>	NBRP* <sup>1</sup>
COTNd	<i>B. subtilis</i> 168 <i>tasA::erm</i>	NBRP* <sup>1</sup>
BKE11550	<i>B. subtilis</i> 168 <i>yjbH::erm</i>	NBRP* <sup>1</sup>
TKSYcomp	pHyjbl1/ BKE11550	This work
TKSY25	pHyjbl4/ BKE11550	This work
TKSY63	pHyjbl5/ BKE11550	This work
TKSY89	pHyjbl6/ BKE11550	This work

Plasmid	Description	Source
pHY300PLK	A vector with <i>hsrM1</i> , <i>leuA8</i> , <i>metB5</i> , and <i>tet</i> for stable gene expression in <i>B. subtilis</i>	TaKaRa Bio
pET28b(+)	An overexpression vector with a T7 promoter and <i>kan</i>	Novagen

pHyjb11	<p>A synthetic <i>yjbI</i> gene fragment<sup>*2</sup>, whose sequence is shown below, was inserted into the EcoRI-BamHI sites of pHY300PLK:</p> <p><b>GAATTCATGGGACAATCCTTTAACGCCCCTTATGAAGCAATCGGTGAAGAACTTTTATCTCAGTTGGTTGACACATTTTACGAACGGTAGCGTCACATCCGCTGCTTAAACCGATTTTCCGAGCGATCTGACAGAAACAGCAAGAAAACAAAAACAGTTTCTGACACAAATCTGGGCGGACCGCCGCTGTATACAGAAGAACATGGCCATCGATGCTTAGAGCTCGCCATTTACCGTTTCCGATTACAAATGACGCGCAGATGCGTGGCTGTCTTGCATGAAAGATGCCATGGATCATGTTGGCCTGGAAGGAGAAATCAGAGAATTTCTTTTGGACGCCTGGAAGTACAGCAAGACATATGGTGAATCAAACGGAAGCCGAAGACAGAAGCAGCTAAGGATCC</b></p>	This work
pHyjb14	<p>A synthetic Y25F <i>yjbI</i> gene fragment<sup>*2</sup>, whose sequence is shown below, was inserted into the EcoRI-BamHI sites of pHY300PLK:</p> <p><b>GAATTCATGGGACAATCGTTTAACGCACCTTATGAAGCGATTGGAGAGGAACTTCTATCGCAACTTGTTGATACTTTTATGAGCGTGTGCGTCTCATCCTTTGCTGAAGCCGATTTTCCAAGCGATTTGACAGAAACCGCCAGGAAACAGAAGCAATTCTTAACTCAGTATTTAGGCGGGCCTCCTCTTTATACTGAGGAACACGGCCATCCTATGCTCAGAGCAAGGCATCTTCCCTTTCCAATTACAAACGAGAGAGCTGATGCGTTTCTCAGCTGTATGAAGGACGCAATGGACCATGTAGGGCTGGAGGGCGAAATTCGTGAGTTTTTGTGGCCGGCTGGAGTTGACAGCAAGGCATATGGTGAATCAAACGGAAGCGGAGGATCGATCATCTTGAGGATCC</b></p>	This work
pHyjb15	<p>A synthetic Y63F <i>yjbI</i> gene fragment<sup>*2</sup>, whose sequence is shown below, was inserted into the EcoRI-BamHI sites of pHY300PLK:</p> <p><b>GAATTCATGGGACAATCGTTTAACGCACCTTATGAAGCGATTGGAGAGGAACTTCTATCGCAACTTGTTGATACTTTTATGAGCGTGTGCGTCTCATCCTTTGCTGAAGCCGATTTTCCAAGCGATTTGACAGAAACCGCCAGGAAACAGAAGCAATTCTTAACTCAGTATTTAGGCGGGCCTCCTCTTTTACTGAGGAACACGGCCATCCTATGCTCAGAGCAAGGCATCTTCCCTTTCCAATTACAAACGAGAGAGCTGATGCGTGGCTCAGCTGTATGAAGGACGCAATGGACCATGTAGGGCTGGAGGGCGAAATTCGTGAGTTTTTGTGGCCGGCTGGAGTTGACAGCAAGGCATATGGTGAATCAAACGGAAGCGGAGGATCGATCATCTTGAGGATCC</b></p>	This work
pHyjb16	<p>A synthetic W89F <i>yjbI</i> gene fragment<sup>*2</sup>, whose sequence is shown below, was inserted into the EcoRI-BamHI sites of pHY300PLK:</p> <p><b>GAATTCATGGGACAATCGTTTAACGCACCTTATGAAGCGATTGGAGAGGAACTTCTATCGCAACTTGTTGATACTTTTATGAGCGTGTGCGTCTCATCCTTTGCTGAAGCCGATTTTCCAAGCGATTTGACAGAAACCGCCAGGAAACAGAAGCAATTCTTAACTCAGTATTTAGGCGGGCCTCCTCTTTATACTGAGGAACACGGCCATCCTATGCTCAGAGCAAGGCATCTTCCCTTTCCAATTACAAACGAGAGAGCTGATGCGTTTCTCAGCTGTATGAAGGACGCAATGGACCATGTAGGGCTGGAGGGCGAAATTCGTGAGTTTTTGTGGCCGGCTGGAGTTGACAGCAAGGCATATGGTGAATCAAACGGAAGCGGAGGATCGATCATCTTGAGGTACC</b></p>	This work

pHtasA1	<p>A synthetic <i>tasA</i> gene fragment<sup>*2</sup>, whose sequence is shown below, was inserted into the EcoRI-BamHI site of pHY300PLK to produce TasA with a C-terminal His<sub>6</sub>-tag (TasA-His):</p> <p><b><u>GAATTC</u>ATGGGAATGAAGAAAAAATTAAGCCTGGGAGTGGCA</b>  TCTGCAGCTTTAGGATTAGCGCTGGTCGGCGGAGGCACATGGG  CTGCATTTAACGATATCAAATCTAAAGATGCAACATTTGCGTC  AGGCACACTTGATTAAAGCGCTAAAGAAAACCTCAGCCAGCGTC  AATTTAAGCAACCTGAAACCGGGAGATAAACTGACAAAAGAT  TTTCAATTTGAAAATAACGGCTCTCTGGCTATCAAAGAAGTTCT  TATGGCCCTGAACTACGGAGATTTTAAAGCAAACGGAGGCTCT  AACACATCACCGGAAGATTTTCTGTACAGTTTGAAGTCACAC  TGCTTACAGTTGGAAAAGAAGGCGGCAATGGCTATCCGAAAA  ACATTATCCTGGATGATGCCAATCTTAAAGATCTGTACCTTATG  TCAGCAAAAAACGATGCAGCGCTGCCGAAAAAATCAAAAAA  CAAATCGATCCGAAATTTCTGAACGCAAGCGGCAAAAGTTAACG  TGGCGACAATTGATGGAAAACAGCTCCGGAATATGATGGCG  TTCCGAAAACACCGACAGATTTTGATCAAGTGCAGATGGAAAT  CCAGTTTAAAGATGATAAAACAAAAGATGAAAAAGGACTTAT  GGTGCAAAACAAATACCAGGGCAACTCTATCAAACCTCAATTT  TCATTTGAAGCGACACAGTGGAAATGGACTGACAATTAAGAAA  GATCATACAGATAAAGATGGCTACGTAAAGAAAAACGAAAAA  GCTCATTGAGAAGATAAAAACCATCATCATCATCATTA<u>AA</u></p>	This work
pEyjbI2	<p>A synthetic <i>yjbI</i> gene fragment<sup>*2</sup>, whose sequence is shown below, was inserted into the NcoI-BamHI site of pET28b(+):</p> <p><b><u>CCATGGG</u>TCAGAGCTTTAACGCGCCGTACGAGGCGATCGGCG</b>  AGGAACTGCTGAGCCAACCTGGTGGACACCTTCTATGAACGTGT  TGCGAGCCACCCGCTGCTGAAGCCGATTTTCCGAGCGATCTG  ACCGAAACCGCGCGTAAGCAGAAACAATTCCTGACCCAGTAC  CTGGGTGGCCCGCCGCTGTATACCGAGGAACACGGTCACCCGA  TGCTGCGTGCGCGTCACCTGCCGTTCCCGATCACCAACGAACG  TGCGGACGCGTGGCTGAGCTGCATGAAAGACGCGATGGATCA  CGTGGGTCTGGAGGGCGAAATTCGTGAGTTCCTGTTTGGCCGT  CTGGAACCTGACCGCGCGTCACATGGTTAACCAAACCGAGGCG  GAAGATCGTAGCAGCT<u>AAAGGATCC</u></p>	This work

958

959 **Figure 2-source data 1.** PVDF membrane after Western blotting treatment of soluble and  
960 insoluble fractions of *B. subtilis* extracts with anti-TasA antibody.

961

962 **Figure 2-source data 2.** Gel image of Fenton reaction-treated TasA after electrophoresis and  
963 silver staining.

964

965 **Figure 2-source data 3.** PVDF membrane after Western blotting treatment of each fraction  
966 of *B. subtilis* using anti-YjbI antiserum.

967

**Figure 2-source data 4.** PVDF membrane after Western blotting treatment of protease-treated *B. subtilis* extracts using anti-Yjbl antiserum.

**Figure 3-source data 1.** Gel image of Fenton reaction-treated BSA after electrophoresis and silver staining.

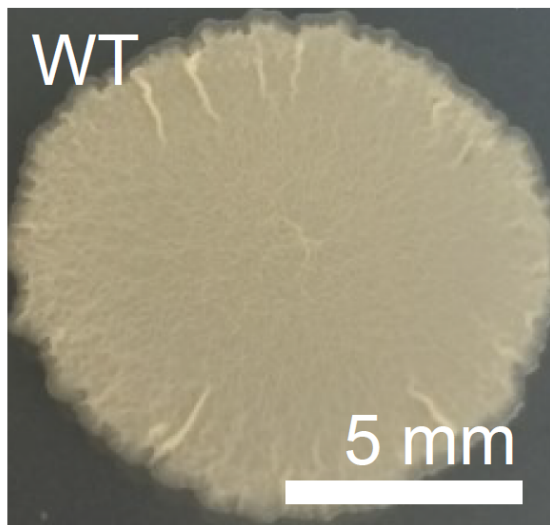
**Figure 3-source data 2.** Gel image of AAPH-treated BSA after electrophoresis and silver staining.

**Figure 3-source data 3.** Gel image of AAPH-treated BSA and haemproteins after electrophoresis and silver staining.

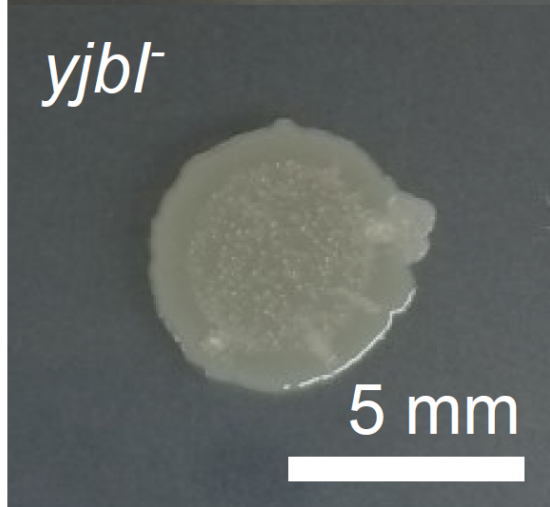
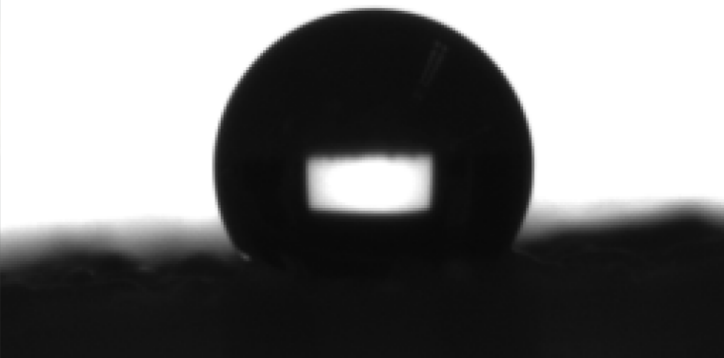
**Figure 2-figure supplement 1 source data.** Gel image of column-purified recombinant Yjbl after electrophoresis.

**Figure 3 figure supplement 1 source data.** Gel image of column-purified recombinant TasA after electrophoresis.

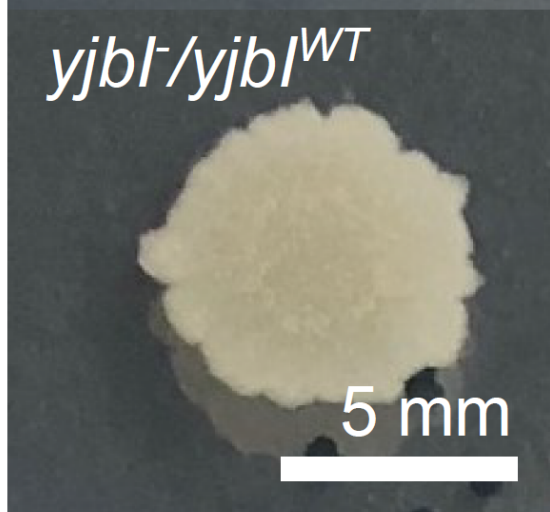
**Figure 4 figure supplement 1 source data.** Gel image of column-purified recombinant Yjbl (Y63F) after electrophoresis.



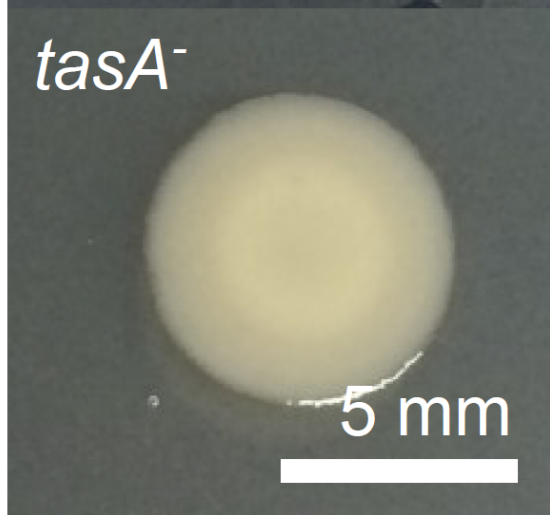
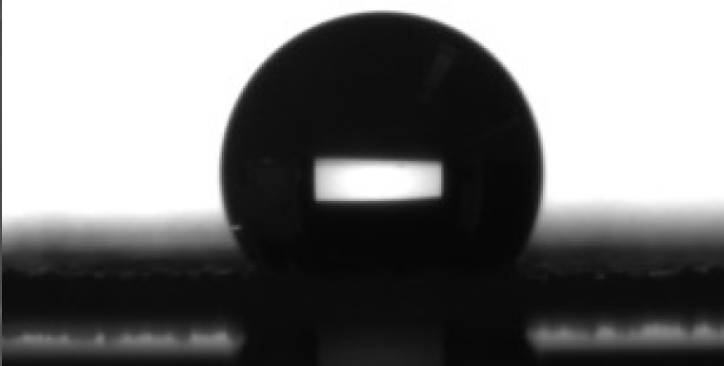
$116 \pm 4.12^\circ$



$30 \pm 1.55^\circ$

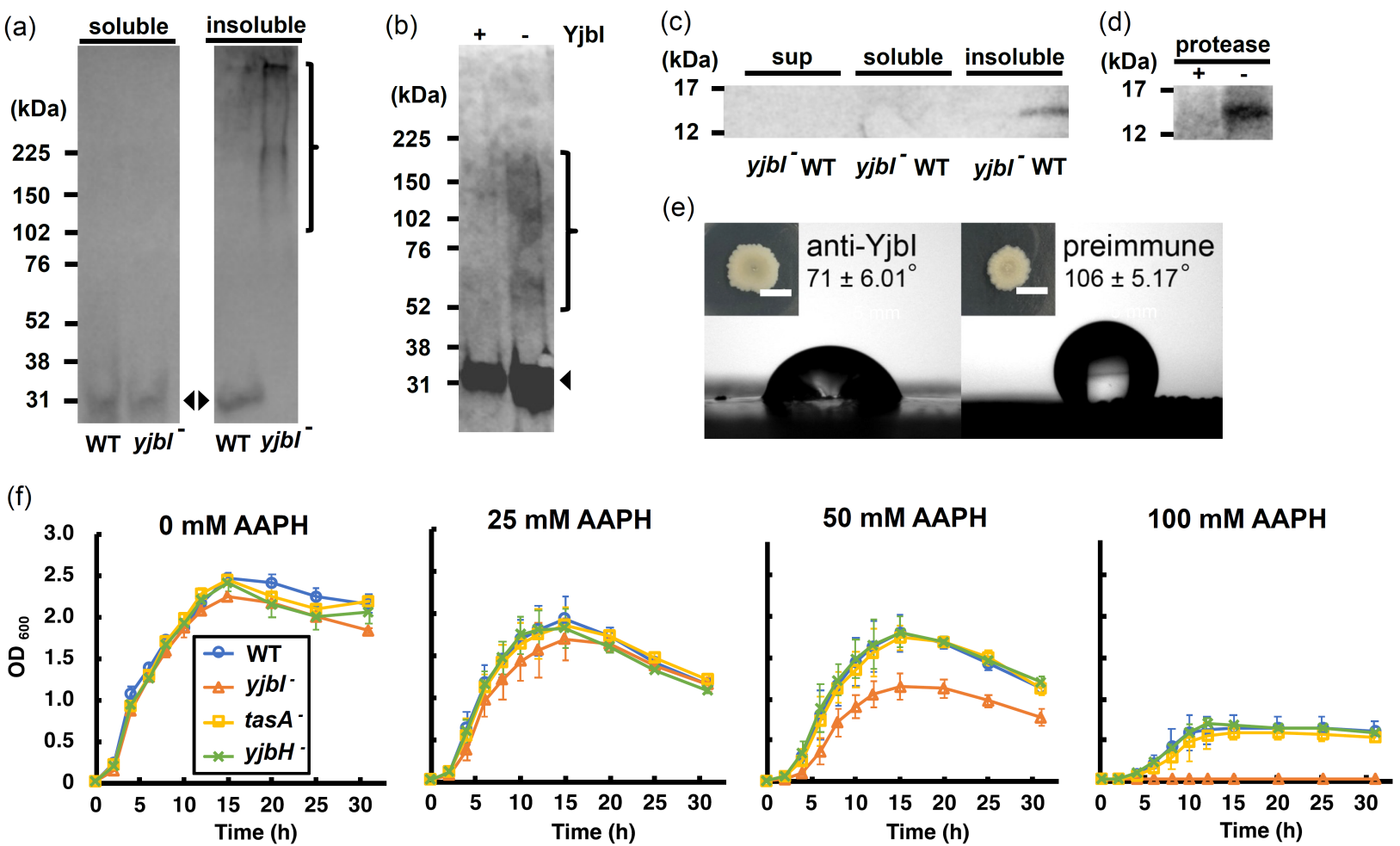


$98 \pm 3.92^\circ$



$13 \pm 3.38^\circ$







(kDa)

225

150

76

52

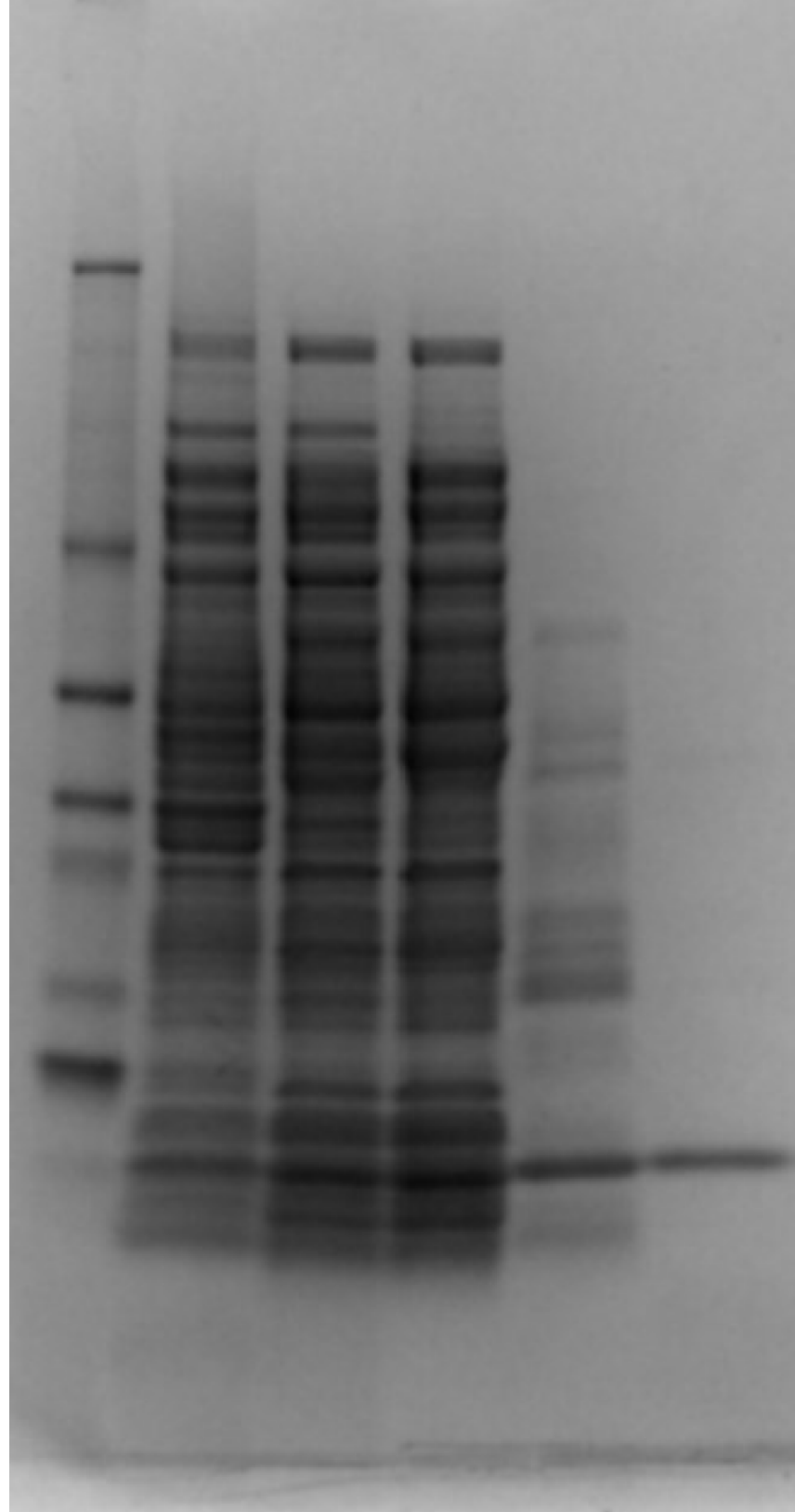
38

31

24

17

12



← Yjbl

M

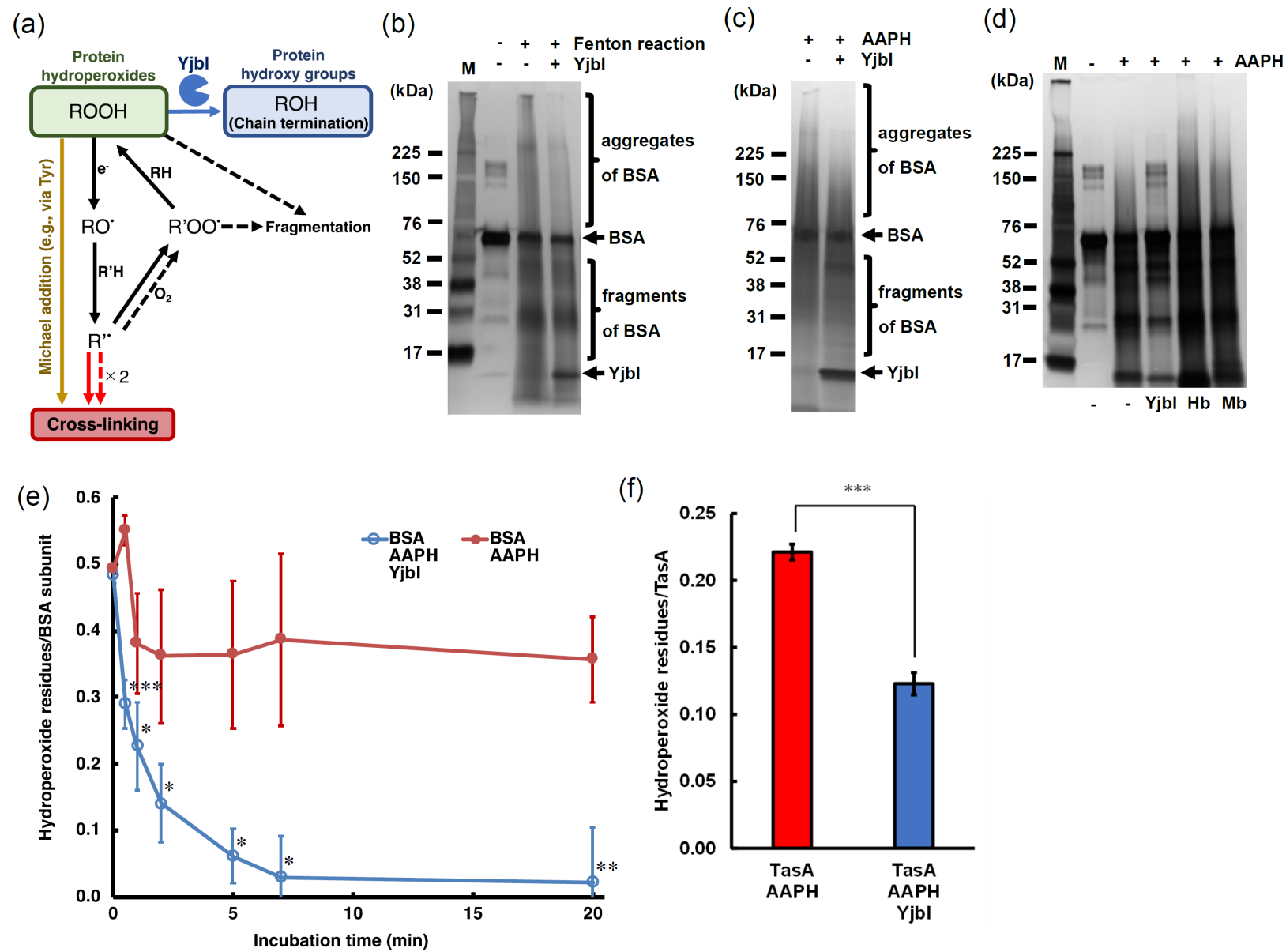
whole-cell

soluble

30-60% AS

gel filtration

DEAE



(kDa)

225—

150—

102—

76—

52—

38—

31—

24—

17—

← Tagged TasA

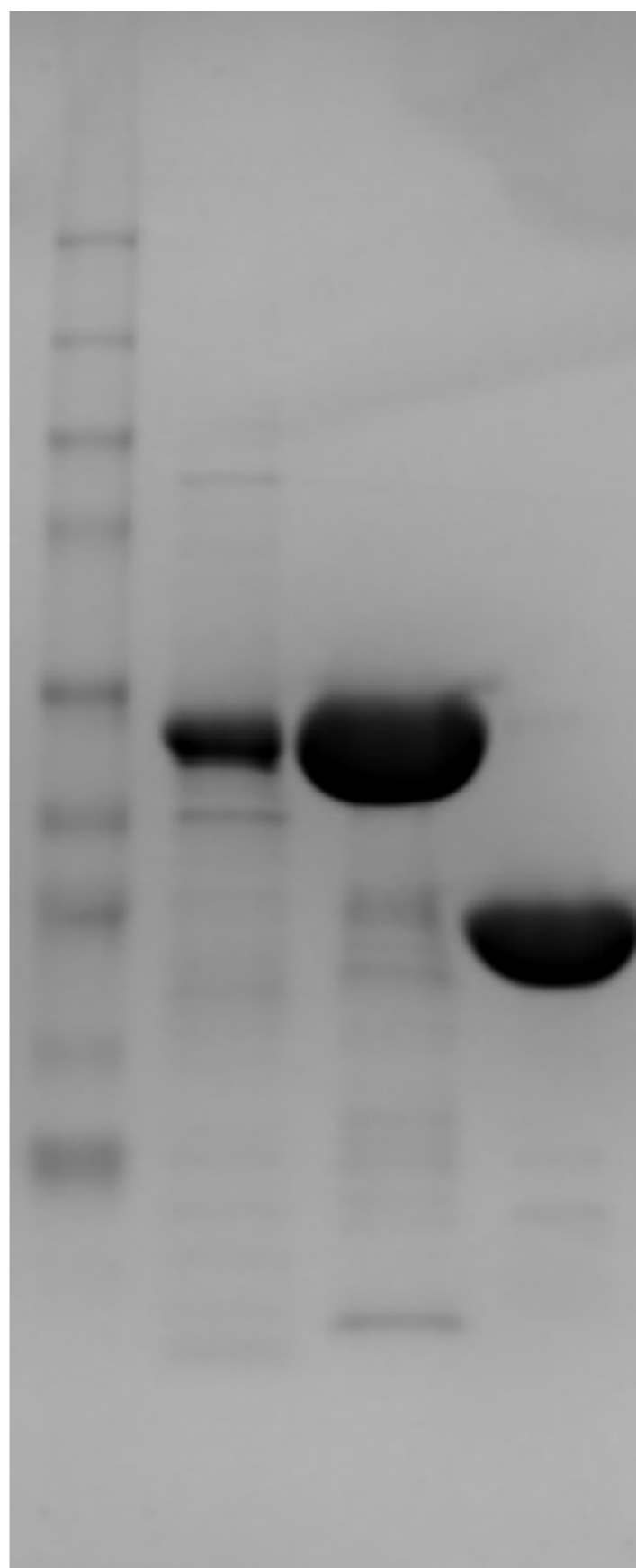
← TasA

M

1

2

3

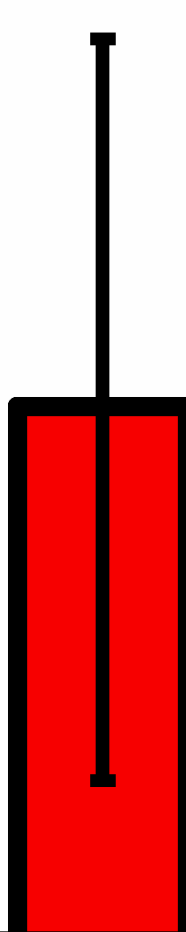
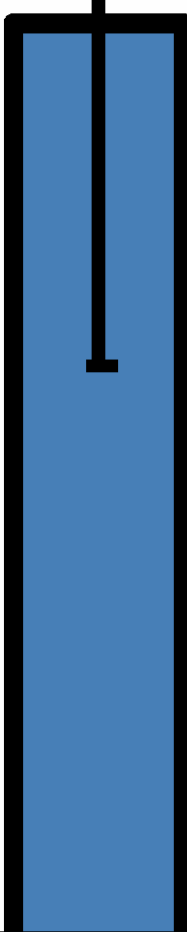


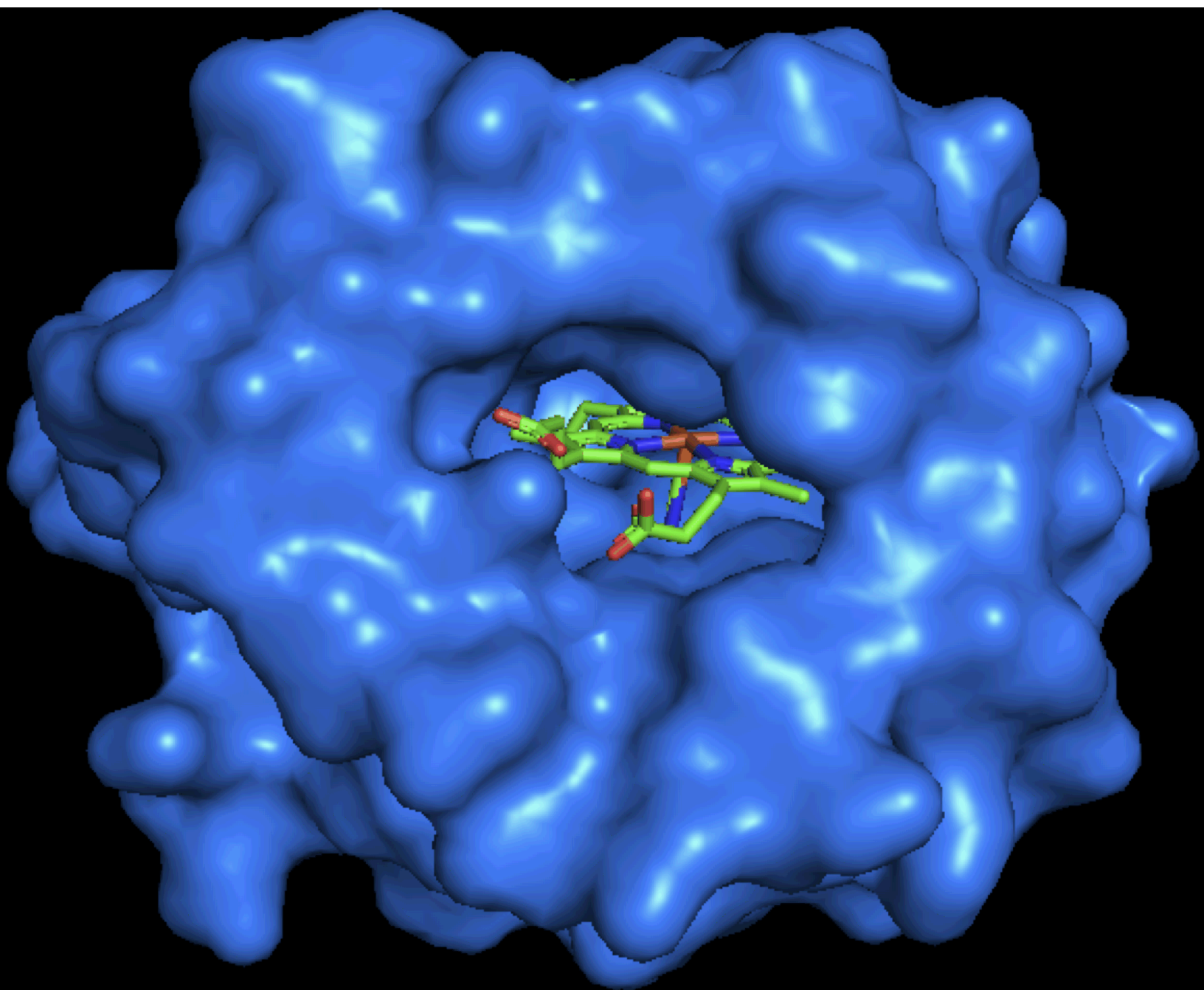
**Amount of lipid hydroperoxide  
(nmol/g biofilm)**

**10.0**  
**8.0**  
**6.0**  
**4.0**  
**2.0**  
**0.0**

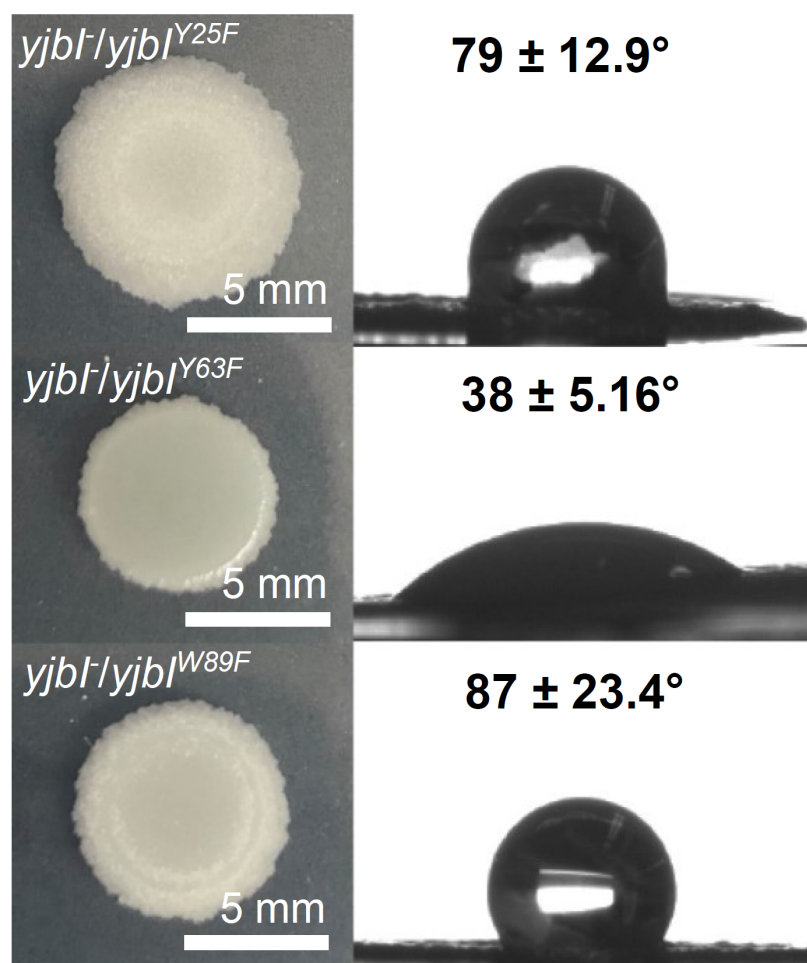
**WT**

***yjbl*<sup>-</sup>**

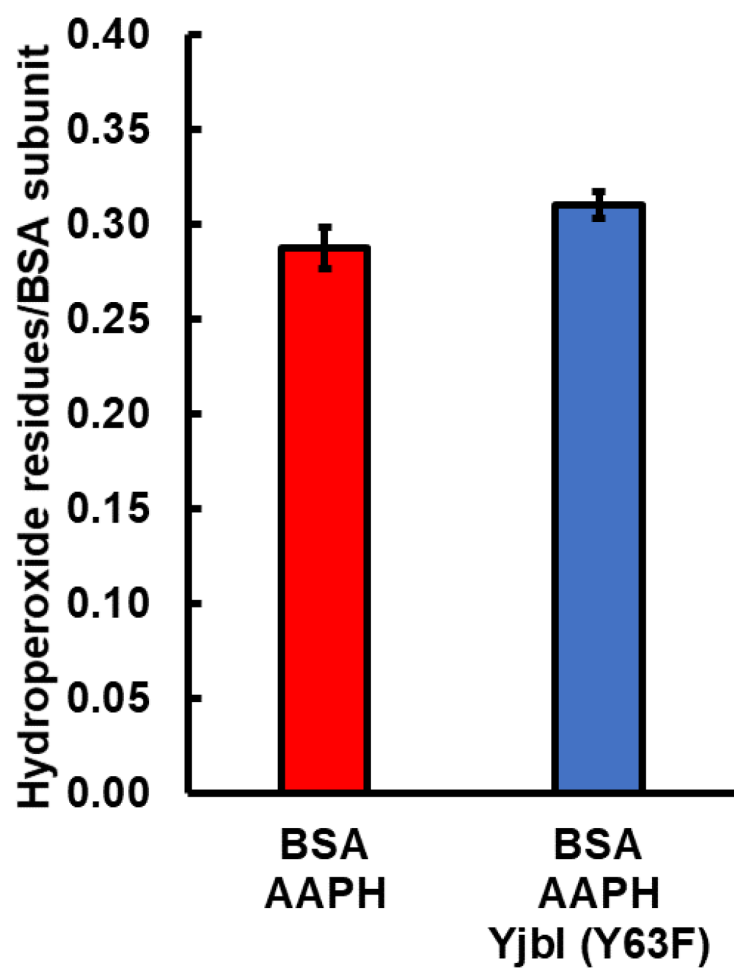




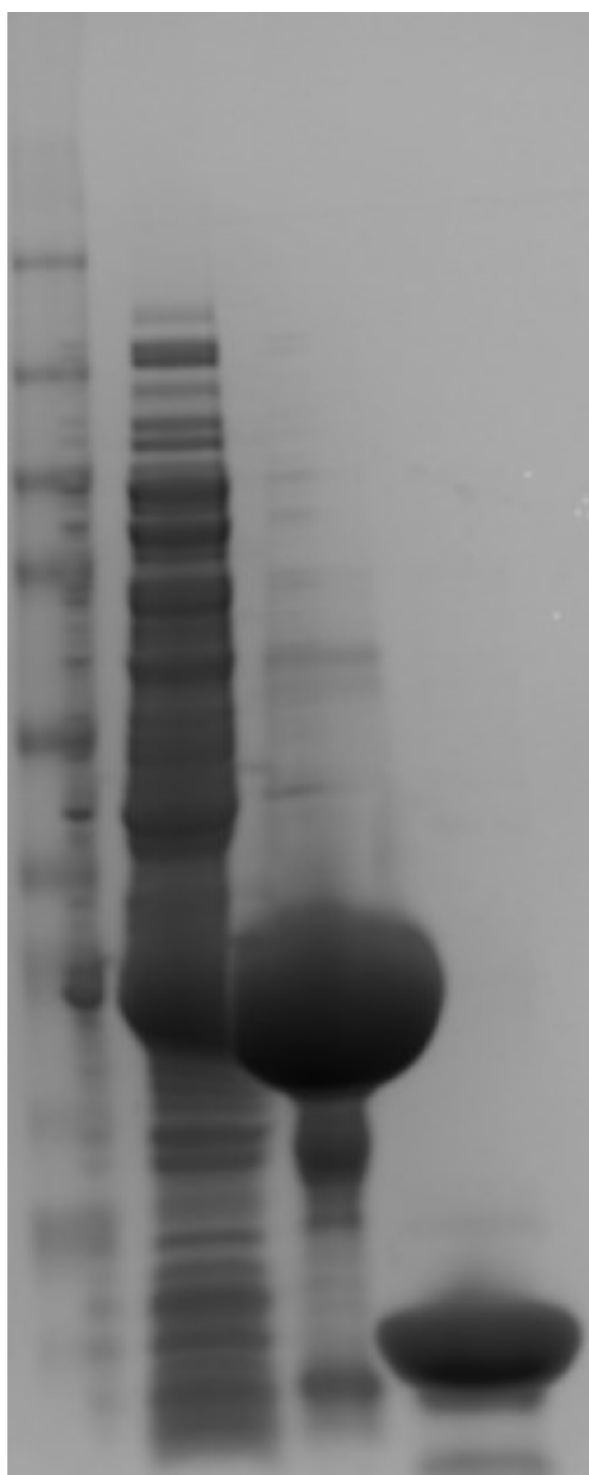
(a)



(b)



225—  
150—  
102—  
76—  
52—  
38—  
31—  
24—  
17—  
12—

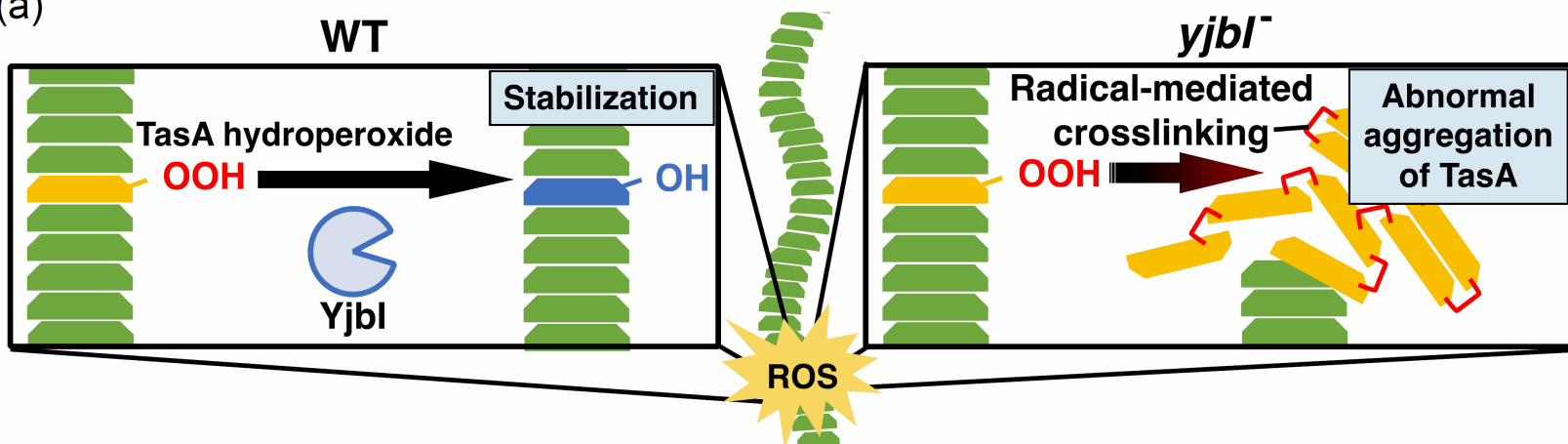


M 1 2 3

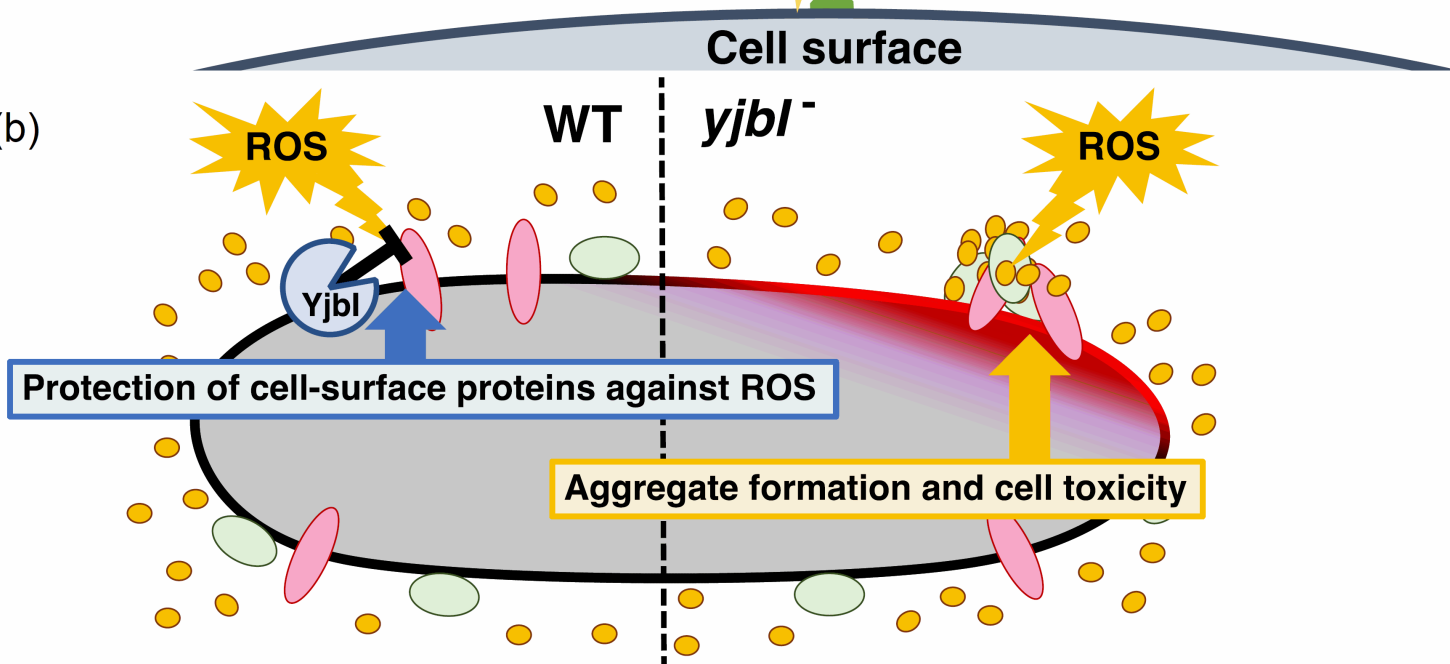
← Tagged Yjbl (Y63F)

← Yjbl (Y63F)

(a)



(b)





**Bacillus subtilis Group II TrHb**

MGQSFNAPYEAIGEELLSQLVDTFYERVASHPLLKPIFPSDLTETARKQKQFLTQYLGGPPLYTEEHGHPMLRAR  
HLPFPITNERADAWLSCMKDAMDHVGLEGEIREFLFGRLELTARHVMVNQTEAEDRSS

**PSORTb Results**

SeqID: seq

Analysis Report:

CMSVM+	Unknown	[No details]
CWSVM+	Unknown	[No details]
CytoSVM+	Cytoplasmic	[No details]
ECSVM+	Unknown	[No details]
ModHMM+	Unknown	[No internal helices found]
Motif+	Unknown	[No motifs found]
Profile+	Unknown	[No matches to profiles found]
SCL-BLAST+	Unknown	[No matches against database]
SCL-BLASTe+	Unknown	[No matches against database]
Signal+	Unknown	[No signal peptide detected]

Localization Scores:

Cytoplasmic	7.50
CytoplasmicMembrane	1.15
Cellwall	0.62
Extracellular	0.73

Final Prediction:

Cytoplasmic	7.50
-------------	------

